# Comparison of Arsenazo III Optical Signals in Intact and Cut Frog Twitch Fibers

JAMES MAYLIE, MALCOLM IRVING, NING LEUNG SIZTO, and W. KNOX CHANDLER

From the Department of Physiology, Yale University School of Medicine, New Haven, Connecticut 06510

ABSTRACT The Ca indicator arsenazo III was introduced into cut frog twitch fibers by diffusion from end-pool segments rendered permeable by saponin. After 2–3 h, the arsenazo III concentration at the optical recording site in the center of a fiber reached two to three times that in the end-pool solutions. Thus, arsenazo III was bound to or taken up by intracellular constituents. The time course of indicator appearance was fitted by equations for diffusion plus linear reversible binding; on average, 0.73 of the indicator was bound and the free diffusion constant was $0.86 \times 10^{-6}$ cm$^2$/s at 18°C. When the indicator was removed from the end pools, it failed to diffuse away from the optical site as rapidly as it had diffused in. The wavelength dependence of resting arsenazo III absorbance was the same in cut fibers and injected intact fibers. After action potential stimulation, the active Ca and dichroic signals were similar in the two preparations, which indicates that arsenazo III undergoes the same changes in absorbance and orientation in both cut and intact fibers. Ca transients in freshly prepared cut fibers appeared to be similar to those in intact fibers. As a cut fiber experiment progressed, however, the Ca signal changed. With action potential stimulation, the half-width of the signal gradually increased, regardless of whether the indicator concentration was increasing or decreasing. This increase was usually not accompanied by any change in the amplitude of the Ca signal at a given indicator concentration or by any obvious deterioration in the electrical condition of the fiber. In voltage-clamp experiments near threshold, the relation between peak [Ca] and voltage usually became less steep with time and shifted to more negative potentials. All these changes were also observed in cut fibers containing antipyrylazo III (Maylie, J., M. Irving, N. L. Sizto, and W. K. Chandler. 1987. *Journal of General Physiology.* 89:83–143). They are considered to represent a progressive change in the physiological state of a cut fiber during the time course of an experiment.

Address reprint requests to Dr. W. Knox Chandler, Department of Physiology, 333 Cedar Street, New Haven, CT 06510. Dr. Irving's present address is Department of Biophysics, King's College London, 26-29 Drury Lane, London WC2B 5RL, England. Dr. Sizto's present address is 3154 Waugh Place, Fremont, CA 94536.

J. GEN. PHYSIOL. © The Rockefeller University Press · 0022-1295/87/01/0041/41 $1.00 

Volume 89 January 1987 41–81

## INTRODUCTION

The preceding article (Irving et al., 1987) described a new apparatus for making rapid optical measurements on single muscle fibers. Changes in the transmitted light intensity at three different wavelengths and two orthogonal linear polarizations can be measured simultaneously on a millisecond time scale. Experiments on freshly prepared cut fibers showed that most of their intrinsic optical properties, resting as well as active, were similar to those of intact fibers. The main exception was that both the resting birefringence and the peak change after an action potential were smaller in cut than in intact fibers. Also, during the time course of an experiment, the active birefringence signal changed to an extent not reported and probably not found in intact fibers.

Other differences between cut and intact fibers have been published. The distribution of intramembranous charge movement in muscle is regulated by membrane voltage in a manner described approximately by a two-state Boltzmann distribution. In frog twitch muscle, the Boltzmann voltage dependence factor is 7–13 mV in intact fibers (Schneider and Chandler, 1973, 1976; Adrian and Almers, 1976; Chandler et al., 1976; Shlevin, 1979; Hui, 1983), but is 15–16 mV, on average, in cut fibers (Horowicz and Schneider, 1981; Luttgau et al., 1983). The strength-duration curve for contraction, however, is similar in cut and intact fibers (Kovacs and Schneider, 1978). The Boltzmann factor for changes in Nile Blue A fluorescence, also in frog twitch muscle, is ~9 mV in cut fibers (Vergara et al., 1978), whereas in intact fibers it is 4–5 mV, at least near threshold (Baylor et al., 1984). Finally, in rat muscle, the curve relating the inactivation variable, $h$, of Na conductance to voltage is usually shifted to more negative potentials in cut than in intact fibers (Pappone, 1980).

For several reasons, described in the Introduction of the preceding article (Irving et al., 1987), we wanted to study intracellular Ca transients in cut rather than intact fibers. Because of the differences between cut and intact fibers described above, we decided to make a systematic comparison of optical Ca signals in the two preparations. Arsenazo III, introduced to physiologists by Brown et al. (1975) and first used in muscle fibers by Miledi et al. (1977), was selected for measuring Ca because it is easy to inject and has been more widely used in frog muscle than any other metallochromic Ca indicator. Arsenazo III has the disadvantage that the optical signals recorded with it are not related in a simple way to the free [Ca] transient. After an increase in myoplasmic [Ca], at least two different Ca:indicator complexes are formed, one almost immediately and another after a 10-ms delay (Baylor et al., 1983*b*; Quinta-Ferreira et al., 1984). Our use of arsenazo III, however, to compare Ca transients in cut and intact fibers, requires only that the indicator behave in the same way in the two preparations.

This article presents a comparison of optical signals from arsenazo III in cut and intact fibers. The primary conclusion is that arsenazo III signals recorded from cut fibers early in an experiment closely resemble those recorded from intact fibers. The similarities include the wavelength dependence of resting absorbance; the time course and amplitude of the Ca signal, as well as its dependence on wavelength and arsenazo III concentration; and the time course,

amplitude, and wavelength dependence of the dichroic signal. Thus, after action potential stimulation, arsenazo III appears to undergo the same changes in absorbance and orientation in a cut fiber that it does in an intact fiber.

Although Ca signals are similar in freshly prepared cut and intact fibers, differences appear as a cut fiber experiment progresses. In voltage-clamp experiments near threshold, for example, the peak amplitude of the Ca transient has the same voltage dependence in a freshly prepared cut fiber as in an intact fiber. During the course of a cut fiber experiment, however, the relation between peak [Ca] and voltage usually becomes less steep and shifts to more negative potentials. Similarly, in action potential experiments, the half-width of the Ca signal increases with the duration of the experiment in cut but not in intact fibers. These changes are also found with antipyrylazo III (Maylie et al., 1987), another Ca indicator, so they are not due simply to a problem with arsenazo III. Rather, it appears that the physiological state of a cut fiber changes during the course of an experiment, perhaps because of changes in the concentration of internal factors that regulate either the release of Ca from the sarcoplasmic reticulum or its subsequent removal from the myoplasm. Such changes could occur by diffusion along the relatively short distance from the central region of a fiber to the end-pool solutions.

## METHODS

The fiber preparation and electrical and optical methods are described in the preceding article (Irving et al., 1987). Except where noted, the experiments were carried out on cut muscle fibers with saponin-treated end-pool regions. Arsenazo III was obtained from Sigma Chemical Co. (St. Louis, MO) and purified by the procedure of Yingst and Hoffman (1978). It was usually introduced into fibers by diffusion from the end pools but was occasionally introduced by ionophoretic injection by microelectrode (Baylor et al., 1982*a*). The frequency of action potential or voltage-clamp stimulation was $\leq$1/min. All active signals were filtered with 0.625-kHz eight-pole Bessel filters. The holding potential was $-90$ mV and the temperature was usually 17–19°C.

### *Measurement of Resting and Active Spectra*

Resting and active spectra were usually measured in mode 1 (Figs. 2 and 3 in Irving et al., 1987). The three interference filters, $\lambda_1$, $\lambda_2$, and $\lambda_3$, were chosen as follows. The $\lambda_3$ filter selected long-wavelength light not absorbed by the indicator; 750 nm was used with arsenazo III. The $\lambda_2$ filter selected a wavelength at which the absorbance of indicator changed when it complexed Ca; for arsenazo III, 660 nm was used. In the first experiments, on intact fibers, these filters had a 10-nm bandpass. In later experiments, on cut fibers, the bandpass was increased to 30 nm to increase the transmitted light intensity and thereby improve the signal-to-noise ratio. In either case, the $\lambda_2$ and $\lambda_3$ filters were mounted before each experiment and could not readily be changed during it. The $\lambda_1$ filter, on the other hand, was easy to change. The standard wavelength for this filter was the isosbestic wavelength of the indicator for changes in pH and Mg, so that the $\lambda_1$ absorbance could be used to estimate the concentration of indicator; for arsenazo III, 570 nm was used. Unless otherwise noted, 10-nm bandpass filters were used in the $\lambda_1$ position.

Measurements of absorbance were corrected for the intrinsic contribution of the fiber as described in the following section. Resting indicator-related spectra were obtained from measurements of absorbance made with different 10-nm filters in the $\lambda_1$ position. Active

Ca spectra were obtained by comparing simultaneously recorded changes in indicator-related $\lambda_1$ and $\lambda_2$ absorbance using a series of filters in the $\lambda_1$ position. If the 660-nm $\lambda_2$ filter had a 30-nm bandpass, as was always the case with cut fibers, the $\lambda_2$ traces were scaled to the magnitude expected for a 10-nm filter. The scaling factor was obtained experimentally by comparing $\lambda_2$ traces, taken with a 30-nm bandpass 660-nm filter, with simultaneously recorded $\lambda_1$ traces, taken with a 10-nm bandpass 660-nm filter.

### *Correction of Absorbance Signals for the Intrinsic Contribution*

The absorbance of a muscle fiber containing an indicator such as arsenazo III consists of an indicator-related component plus a component intrinsic to the fiber. In all experiments, resting intrinsic absorbance was measured at selected wavelengths before the indicator diffused into the fiber. Values at other wavelengths were estimated from the empirical equation

$$A(\lambda) = a + b(550 \text{ nm}/\lambda)^m, \tag{1}$$

which is given in the preceding article (Eq. 19 in Irving et al., 1987). If data were taken at fewer than five wavelengths, $m$ could not be determined reliably and hence was set equal to 4.5, the average value from early measurements. This value is slightly different from the final value, 4.1, given in Table III of Irving et al. (1987), but not sufficiently different to require redoing the analysis.

During the course of an experiment, with or without an indicator present, the intrinsic absorbance usually changes somewhat. If an indicator is used, such changes can be monitored with long-wavelength light not absorbed by the indicator. We assumed that such absorbance changes were independent of wavelength (and thus attributable to a change in $a$ in Eq. 1), as found in two out of three fibers studied without an indicator (Irving et al., 1987). At any time during an experiment with an indicator, then, the intrinsic absorbance was estimated as the initial intrinsic absorbance, either measured or calculated from Eq. 1, plus the change in long-wavelength absorbance.

The calculation of resting absorbance from the intensity of transmitted light requires knowing the intensity of incident light (Eqs. 1 and 7 in Irving et al., 1987). This was determined by linearly interpolating between measurements made at the beginning and end of an experiment, with the fiber moved laterally out of the light path; in the average experiment, light intensity decreased 0.54% in 154 min (Irving et al., 1987). If the intensity did not change at a constant rate, an error would be introduced into the calculation. Such errors in indicator-related absorbance would be automatically removed, however, by the procedure for estimating changes in intrinsic absorbance, provided there were no spectral changes in the incident light.

The active intrinsic component of $\Delta A(\lambda, 1{:}2)$ or $\Delta A(\lambda, 1{:}1)$ was estimated on the assumption that it has the same time course at different wavelengths and an amplitude that varies according to

$$\Delta A(\lambda) \propto \lambda^{-n}, \tag{2}$$

as found in the preceding article (Irving et al., 1987). Since both the amplitude of the intrinsic signal at a fixed wavelength and the parameter $n$ can change during an experiment (Irving et al., 1987), it is necessary to monitor both throughout an experiment, even after an indicator has been introduced. The method for doing this with arsenazo III is illustrated in Fig. 4 and described in the Results.

All measurements of $A(\lambda)$ and $\Delta A(\lambda)$ in this article have been corrected for intrinsic contributions except for the traces in Figs. 4, *A* and *B*, 16, *A* and *B*, and 19*A* (750-nm traces only).

### *Measurement of Arsenazo III Concentration*

The myoplasmic concentration, $c$, of arsenazo III was estimated from Beer's law,

$$A(\lambda) = \epsilon(\lambda)cl, \tag{3}$$

using measurements of either indicator-related $A(570, 1{:}2)$, mode 1 recording, or $A(570, 1{:}1)$, mode 2 recording. According to Kendrick et al. (1977), the molar extinction coefficient $\epsilon(570)$ is $3.0 \times 10^4$ $M^{-1}$ $cm^{-1}$; this value, assumed to be independent of the indicator concentration, was used for absorbance measurements made with our 10-nm bandpass 570-nm filter. For the purpose of calculating its concentration, the indicator was assumed to be confined to myoplasmic water. The path length, $l$, was estimated to equal the fiber diameter, determined each time by interpolation between measurements made during the experiment, multiplied by 0.7; this factor is an estimate of the fraction of muscle volume occupied by myoplasmic water rather than by filaments, sarcoplasmic reticulum, or mitochondria (Baylor et al., 1983*a*).

## RESULTS

### *Viability of Cut Muscle Fibers during the Course of an Experiment*

13 experiments were carried out on cut (saponin-treated) fibers in which arsenazo III was introduced either by diffusion from the two end pools (10 fibers) or by ionophoretic injection from a microelectrode (3 fibers). With either method, we wanted an objective assessment of fiber viability during each experiment. This was especially important since, as shown below, the half-width of the Ca signal in cut fibers increased progressively with time in a manner not observed in intact fibers.

The criteria selected for fiber viability were electrical ones: action potential amplitude (not applicable to voltage-clamp experiments), holding current, $r_m$, and $r_e/(r_e + r_i)$. An experiment was terminated when any of these began to show signs of significant deterioration. Columns 5–8 of Table I show early and final measurements of the four parameters. On the whole, the fibers showed only slight deterioration in electrical properties over relatively long periods of time (2–5 h).

Fiber diameter was also measured. In 11 experiments it decreased and in 2 experiments it increased (Table I, column 4); on average, there was a 7.2% decrease over periods varying from 96 to 305 min.

### *Diffusion of Arsenazo III in Cut Muscle Fibers*

*Analysis including reversible binding.* Arsenazo III diffused easily into cut fibers and could be detected at the site of optical recording in the central-pool region within 10–20 min of addition to the end pools. Fig. 1 shows the time course of arsenazo III concentration at the optical recording site in three fibers from the same frog. To minimize any effects on diffusion produced by muscle activation, no more than five stimuli were given during a single experiment. At zero time, 0.5 mM arsenazo III was added to both end pools and thereafter its concentration in the middle of the fiber was monitored optically. In *A* and *B*, the indicator remained in the end pools for the duration of the experiment, whereas in *C* it was removed after 43.3 min. Throughout this article, the period when

the indicator was present in the end pools in pulsed-exposure experiments is indicated by a horizontal bar at the top of each plot.

In all three fibers in Fig. 1, the concentration of arsenazo III at the optical recording site eventually exceeded that in the end pools. This could not happen if all the indicator were freely dissolved in myoplasm. In *A* and *B*, the increase was threefold. Thus, most of the indicator must have been bound to intracellular constituents, taken up by internal compartments, or in some other way concentrated inside the fiber. In the rest of this article, we shall refer to indicator that is not freely dissolved in myoplasmic solution as bound indicator.

TABLE I

*Change of Electrical Parameters during the Time Course of Experiments on Cut Muscle Fibers Containing Arsenazo III*

| (1) Fiber reference | (2) Duration of experiment | (3) Temperature | (4) Diameter | (5) Action potential | (6) Holding current | (7) $r_m$ | (8) $r_e/(r_e + r_i)$ |
|---|---|---|---|---|---|---|---|
| | *min* | *°C* | *μm* | *mV* | *−nA* | *MΩ·cm* | |
| 060684.1 | 96 | 17.7–18.1 | 90–82 | 134–132 | 75–86 | 0.097–0.098 | 0.967–0.961 |
| 060684.2 | 153 | 18.1–17.3 | 98–94 | 132–132 | 75–74 | 0.088–0.077 | 0.966–0.963 |
| 060784.2 | 151 | 17.9–18.0 | 110–116 | 135–134 | 66–71 | 0.069–0.057 | 0.977–0.975 |
| 070284.1* | 166 | 19.0–19.1 | 77–73 | 132–131 | 40–47 | 0.105–0.104 | 0.975–0.968 |
| 070284.2‡ | 108 | 18.9–18.5 | 99–106 | 130–127 | 120–123 | 0.067–0.062 | 0.951–0.954 |
| 070284.3 | 234 | 17.9–18.6 | 89–86 | 135–NR | 35–44 | 0.093–NR | 0.976–NR |
| 092884.1 (I) | 186 | 17.9–17.2 | 78–63 | 133–124 | 50–66 | 0.093–0.074 | 0.963–0.944 |
| 092884.2 (I) | 143 | 18.1–18.0 | 101–92 | 136–129 | 33–74 | 0.069–0.043 | 0.977–0.971 |
| 100184.1 | 222 | 18.6–18.0 | 102–93 | 136–131 | 25–41 | 0.083–0.055 | 0.988–0.980 |
| 100184.2 (I) | 198 | 18.3–18.3 | 118–109 | 134–131 | 71–90 | 0.045–0.044 | 0.978–0.971 |
| 100284.1 | 123 | 17.8–18.0 | 90–78 | 137–134 | 46–59 | 0.099–0.074 | 0.972–0.959 |
| 101284.2 | 305 | 18.4–18.1 | 80–68 | (VC) | 31–53 | 0.188–0.141 | 0.981–0.964 |
| 101584.1 | 277 | 18.1–18.4 | 90–80 | (VC) | 29–38 | 0.235–0.154 | 0.984–0.978 |

Column 1 gives fiber reference and column 2 gives the duration of the experiment beginning from the time of saponin treatment. Columns 3–8 give temperature, fiber diameter, action potential amplitude (measured on the storage oscilloscope), holding current (sign reversed), $r_m$, and $r_e/(r_e + r_i)$; within each column, the first value was obtained ~20 min after saponin treatment and the second value was obtained at the end of the experiment. Sarcomere spacing, 3.7–4.2 μm; holding potential, −90 mV; first 11 fibers, Ringer's solution; last 2 fibers, TEA solution (containing 1 μM tetrodotoxin).

*,‡ Final set of values in columns 5–8, taken 114 and 76 min after saponin treatment, respectively.

NR, not recorded. I, experiment in which arsenazo III was injected. VC, voltage-clamp experiment.

The time course of the indicator concentration (Fig. 1) depends on the rate of diffusion and the characteristics of binding. The simplest assumption for binding is that the amount of bound indicator, $S^*$, is directly proportional at any time to the concentration of indicator, $C^*$, that is free to diffuse:

$$S^* = RC^*. \tag{4}$$

This case is described in Crank (1956). The incorporation of Eq. 4 into the usual one-dimensional diffusion equation gives

$$\frac{\partial C^*}{\partial t} = \frac{D}{R + 1} \frac{\partial^2 C^*}{\partial x^2}, \tag{5}$$

in which $D$ is the true diffusion constant of free indicator and $D/(R + 1)$ is the apparent diffusion constant. The freely diffusing concentration, $C^*$, of indicator

at the center of the optical site, in the middle of the fiber in the central pool, is denoted by $C$ and is obtained by solving Eq. 5 for the appropriate boundary and initial conditions. It is given by Eq. 4.17 in Crank (1956, p. 45) (with $x = 0$):

$$C/C_1 = 1 - \frac{4}{\pi}\sum_{n=0}^{\infty}\frac{(-1)^n}{2n+1}\exp\left[\frac{-D(2n+1)^2\pi^2 t}{4(R+1)L^2}\right]. \quad (6)$$

$C_1$ is the concentration of indicator added to the end pools at $t = 0$ and $L$ is the diffusion path length, taken to be 550 $\mu$m in saponin-treated fibers (300 $\mu$m under the Vaseline seal plus 250 $\mu$m to the middle of the fiber in the central

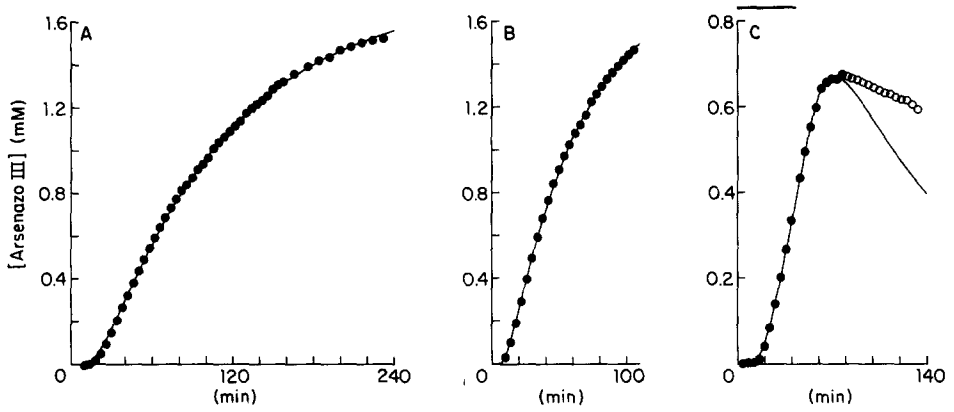


FIGURE 1. Diffusion of arsenazo III in cut muscle fibers and analysis including reversible binding. Panels *A–C* show indicator concentration at the site of optical recording plotted as a function of time after the addition of 0.5 mM arsenazo III to the end pools. In this and subsequent figures, the concentration of arsenazo III, $c$, was estimated from the indicator-related $A(570, 1{:}1)$ or $A(570, 1{:}2)$ using Eq. 3. In *A* and *B*, the indicator was in the end pools during the entire experiment, whereas in *C* it was present for only 43.3 min, as indicated by the horizontal bar. The curves represent least-squares fits of Eqs. 6 and 8 using the filled experimental points only. The fitted parameters are given in columns 4 and 5 of Table II. (*A*) Fiber 070284.3; sarcomere spacing, 3.7 $\mu$m; (*B*) fiber 070284.2; sarcomere spacing, 3.7 $\mu$m; (*C*) fiber 070284.1; sarcomere spacing, 4.2 $\mu$m. All three fibers were from the same frog; the fiber used in *A* was from an iliofibularis muscle and the fibers in *B* and *C* were from one semitendinosus muscle; the indicator was added 2–33 min after saponin treatment. Additional details are given in Table I.

pool). The initial concentration inside the fiber is zero. The total concentration, $c$, of indicator at the center of the optical site is given by

$$c = C + S \quad (7)$$

$$= (R + 1)C. \quad (8)$$

The continuous curves in Fig. 1, *A* and *B*, are least-squares fits of Eqs. 6 and 8 to the experimental points. The parameter $D/(R + 1)$ was found by successive iterations and $(R + 1)$ was found by scaling. The values for these parameters are given in Table II, columns 4 and 5; the diffusion constant, $D$, is given in column 6.

Although the two fibers in *A* and *B* were taken from the same frog, the fitted values of $D/(R + 1)$ were somewhat different: $0.214 \times 10^{-6}$ cm$^2$/s in *A* and $0.386 \times 10^{-6}$ cm$^2$/s in *B*; the ability to bind indicator was similar: $(R + 1) = 3.469$ in *A* and 3.551 in *B*. This example is atypical; usually, with arsenazo III or other indicators, fibers from the same frog gave similar values for both $D/(R + 1)$ and $(R + 1)$.

Fig. 1*C* shows a pulsed-exposure experiment in which arsenazo III was removed from the end pools after 43.3 min. The theoretical curve was calculated by applying the principle of superposition and adding two solutions of Eq. 5, one

TABLE II

*Parameters Associated with the Analysis of Arsenazo III Diffusion in Cut Fibers, Including Reversible Binding*

| (1) Fiber reference | (2) Indicator concentration | (3) Indicator exposure | (4) $D/(R + 1)$ | (5) $(R + 1)$ | (6) $D$ |
|---|---|---|---|---|---|
| | *mM* | *min* | $\times 10^{-6}$ *cm$^2$/s* | | $\times 10^{-6}$ *cm$^2$/s* |
| 060684.1 | 0.5 | 24 | 0.254 | 3.680 | 0.935 |
| 060684.2 (5*A*) | 0.5 | 26 | 0.249 | 3.560 | 0.886 |
| 060784.2 | 0.5 | 38 | 0.247 | 3.437 | 0.849 |
| 070284.1 (1*C*) | 0.5 | 43 | 0.193 | 4.622 | 0.892 |
| 070284.2 (1*B*) | 0.5 | 106 | 0.386 | 3.551 | 1.371 |
| 070284.3 (1*A*) | 0.5 | 232 | 0.214 | 3.469 | 0.742 |
| 100184.1 (7*A*) | 1.0 | 203 | 0.185 | 3.536 | 0.654 |
| 100284.1 | 1.0 | 52 | 0.126 | 4.933 | 0.622 |
| 101284.2 | 1.0 | 33 | 0.230 | 3.193 | 0.734 |
| 101584.1 | 1.0 | 28 | 0.282 | 3.192 | 0.900 |
| Mean | | | 0.237 | 3.717 | 0.859 |
| SEM | | | 0.022 | 0.185 | 0.067 |

Column 1 gives fiber reference; the numbers and letters in parentheses refer to the figures in which theoretical diffusion curves are shown. Column 2 gives the concentration of indicator used in the end pools and column 3 gives the period of time it was present. Columns 4 and 5 give parameters associated with fitting Eqs. 6 and 8 to the experimental points; column 6 gives the product of columns 4 and 5. Indicator was added to the end pools 2–33 min (average value, 12 min) after saponin treatment. In pulsed-exposure experiments, the data points used for fitting the equations were arbitrarily limited to the time period up to and slightly past the peak, so that a good theoretical fit to the early experimental points would be made (see Fig. 1*C*). Fiber information is given in Table I. Sarcomere spacing, 3.7–4.2 μm; average temperature, 18.2°C.

for a step in the end-pool concentration from 0 to $C_1$ at $t = 0$ and the other for a step from 0 to $-C_1$ at $t = 43.3$ min. Only the early points, indicated by filled circles (a convention used throughout this article), were used to determine $D/(R + 1)$ and $(R + 1)$. Later points were not well fitted by the curve. When all the points were used (not shown), neither early nor late points were well fitted. This inability to fit both early and late points was found in all seven fibers in which a pulsed exposure to the indicator was used.

Fitted parameters from 10 fibers, 3 studied with maintained exposure to indicator and 7 with pulsed exposure, are given in Table II. In the pulsed-exposure experiments, only early concentration points were used for the fits.

The average values are $D/(R + 1) = 0.237 \times 10^{-6}$ cm$^2$/s, $(R + 1) = 3.717$, and $D = 0.859 \times 10^{-6}$ cm$^2$/s; these values apply to the ability of arsenazo III to diffuse into rather than out of fibers.

The main conclusion from these experiments is that arsenazo III readily diffuses into cut fibers but that, once inside, most of it becomes bound to intracellular constituents. The simple diffusion plus nonsaturating, equilibrium binding theory used above (Eqs. 4–8) fails to describe the time course of arsenazo III concentration in pulsed-exposure experiments; otherwise, theoretical curves similar to that in Fig. 1*C* would fit data at late times. It appears that indicator diffuses into a fiber more rapidly than it diffuses out. We therefore considered the possibility of irreversible as well as reversible binding.

*Analysis including reversible and irreversible binding.* This section considers diffusion of indicator combined with the simplest kind of reversible plus irreversible binding. Eq. 5 is modified to include a term for linear irreversible binding:

$$\frac{\partial C^*}{\partial t} = \frac{D}{R + 1}\frac{\partial^2 C^*}{\partial x^2} - \frac{k}{R + 1}C^*, \tag{9}$$

in which $k$ is the rate constant associated with irreversible binding. This equation can be solved to give the concentration in the middle of the fiber in the central region:

$$C = \frac{k}{R + 1}\int_0^t C'\exp\left(-\frac{kt'}{R + 1}\right)dt' + C'\exp\left(-\frac{kt}{R + 1}\right), \tag{10}$$

in which $C'$ is equated formally with $C$ in Eq. 6 (Crank, 1956). The measured concentration of indicator is given by

$$c = (R + 1)C + k\int_0^t C dt'. \tag{11}$$

Fig. 2*A* shows the same concentration data as in Fig. 1*C*, but here the continuous curve is the best least-squares fit calculated from Eqs. 10 and 11. The parameters $D/(R + 1)$ and $k/(R + 1)$ were determined by iteration and $(R + 1)$ was determined by scaling. The dashed curve represents the concentration of free plus reversibly bound indicator (first term on the right-hand side of Eq. 11); the dotted curve represents the concentration of irreversibly bound indicator (second term on the right-hand side of Eq. 11). Fig. 2*B* shows data from another pulsed-exposure experiment with the fitted curves from Eqs. 10 and 11; the fit from Eqs. 6 and 8 for linear reversible binding is shown in Fig. 5*A*. The continuous theoretical curves in Fig. 2 provide good fits to the data, whereas those in Figs. 1*C* and 5*A* do not.

Eqs. 10 and 11 were not fitted to data from maintained-exposure experiments. With this protocol, the curves calculated from Eqs. 6 and 8 already provide reasonable fits to the experimental points (Figs. 1, *A* and *B*, and 7*A*), so that the extra parameter, $k$, cannot be estimated reliably.

Concentration data from seven pulsed-exposure experiments were analyzed under the assumption of reversible plus irreversible binding. Whereas reversible binding alone (Eqs. 6 and 8) gave poor fits, as mentioned above, reversible plus irreversible binding (Eqs. 10 and 11) gave fits that were reasonable, although

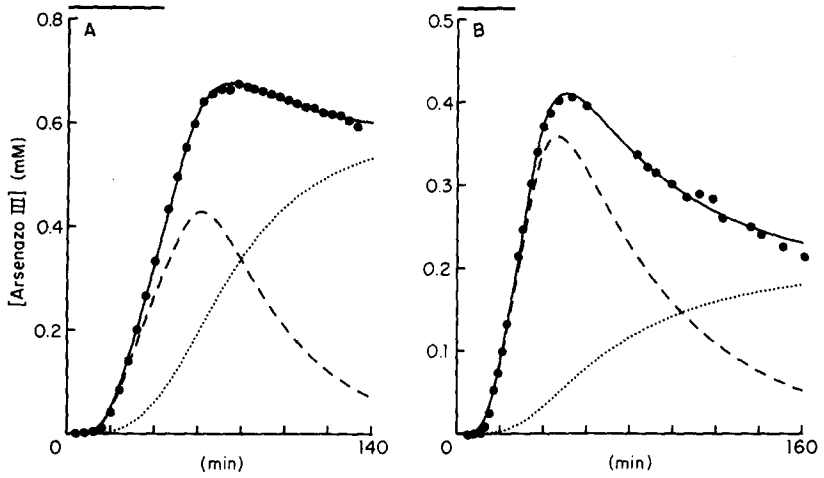


FIGURE 2. Theoretical fits of arsenazo III diffusion in cut muscle fibers, assuming reversible and irreversible binding. (*A*) Data from Fig. 1*C*; (*B*) data from Fig. 5*A*. The continuous curves represent theoretical fits of Eqs. 10 and 11 using all experimental points. The dashed and dotted curves represent, respectively, free plus reversibly bound indicator [$= (R + 1)C$] and irreversibly bound indicator [$= k \int_0^t Cdt'$]. The parameters used for the fits are given in Table III.

not always as good as those in Fig. 2. Table III gives values of $D/(R + 1)$, $(R + 1)$, $D$, $k/(R + 1)$, and $k$. Compared with reversible binding alone (Table II), the addition of an irreversible component increases, on average, the values of both $(R + 1)$, from 3.717 to 5.556, and $D$, from $0.859 \times 10^{-6}$ to $1.089 \times 10^{-6}$ cm$^2$/s.

TABLE III

*Parameters Associated with the Analysis of Arsenazo III Diffusion in Cut Fibers, Including Reversible and Irreversible Binding*

| (1) Fiber reference | (2) $D/(R + 1)$ | (3) $(R + 1)$ | (4) $D$ | (5) $k/(R + 1)$ | (6) $k$ |
|---|---|---|---|---|---|
| | $\times 10^{-6}$ cm$^2$/s | | $\times 10^{-6}$ cm$^2$/s | $\times 10^{-3}$/s | $\times 10^{-3}$/s |
| 060684.1 | 0.254 | 4.676 | 1.188 | 0.30 | 1.40 |
| 060684.2 (2*B*) | 0.245 | 4.015 | 0.984 | 0.11 | 0.45 |
| 060784.2 | 0.237 | 4.412 | 1.046 | 0.22 | 0.96 |
| 070284.1 (2*A*) | 0.187 | 6.797 | 1.271 | 0.31 | 2.10 |
| 100284.1 | 0.117 | 10.069 | 1.178 | 0.35 | 3.49 |
| 101284.2 | 0.209 | 4.232 | 0.884 | 0.16 | 0.67 |
| 101584.1 | 0.229 | 4.695 | 1.075 | 0.13 | 0.63 |
| Mean | 0.211 | 5.556 | 1.089 | 0.23 | 1.39 |
| SEM | 0.018 | 0.829 | 0.050 | 0.04 | 0.41 |

Column 1 gives fiber reference; the numbers and letters in parentheses refer to the figures in which theoretical diffusion curves are shown. Columns 2, 3, and 5 give parameters associated with fitting Eqs. 10 and 11 to the experimental points. Column 4 gives the product of columns 2 and 3, and column 6 gives the product of columns 5 and 3. Indicator was added to the end pools 2–33 min (average value, 14 min) after saponin treatment. Only pulsed-exposure experiments were analyzed in this table and all experimental points were used in making the fits. Additional information is given in Tables I and II. Sarcomere spacing, 3.7–4.2 μm; average temperature, 18.1°C.

The average value of $k$, $1.39 \times 10^{-3}$ $s^{-1}$, corresponds to a time constant of 12 min for irreversible uptake. These results seem consistent with the idea that arsenazo III can be bound both reversibly and irreversibly.

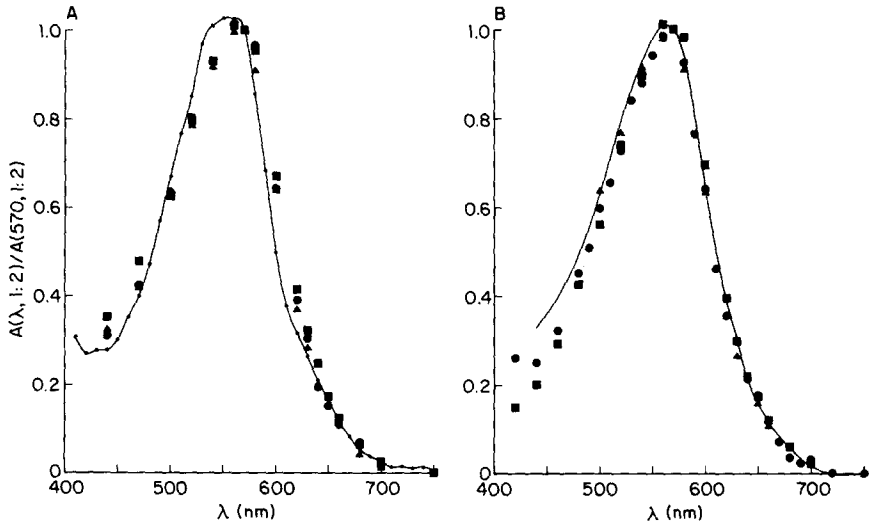


FIGURE 3. Comparison of resting arsenazo III absorbance in intact and cut muscle fibers. In both panels, $A(\lambda, 1{:}2)$, divided by $A(570, 1{:}2)$, has been plotted against wavelength. (*A*) Data from three intact fibers in Ringer's solution. (●) Fiber 041583.2; sarcomere spacing, 4.0 μm; indicator concentration, 0.704–0.471 mM; temperature, 15.8–16.2°C. (■) Fiber 042083.1; sarcomere spacing, 4.0 μm; indicator concentration, 1.001–0.824 mM; temperature, 16.9–17.0°C. (▲) Fiber 050383.1; sarcomere spacing, 4.2 μm; indicator concentration, 0.920–0.791 mM; temperature, 17.2–17.4°C. The small dots, connected by a continuous curve drawn using a cubic spline function (Greville, 1968), are calibration measurements made on the apparatus using a 100-μm cuvette containing 110 mM KCl, 1.08 mM $MgCl_2$, 0.5 mM EGTA, 0.5 mM arsenazo III, and 10 mM PIPES titrated with KOH to pH 6.9; temperature, 25°C. (*B*) Data from three cut fibers in Ringer's solution. (●) Fiber 060684.1; sarcomere spacing, 4.0 μm; indicator concentration, 0.373–0.395 mM; temperature, 18.0°C; time after saponin treatment, 55–61 min. (■) Fiber 060684.2; sarcomere spacing, 4.1 μm; indicator concentration, 0.315–0.289 mM; temperature, 17.2°C; time after saponin treatment, 94–114 min. (▲) Fiber 060784.2; sarcomere spacing, 3.7 μm; indicator concentration, 0.538–0.520 mM; temperature, 17.8°C; time after saponin treatment, 65–85 min. The continuous curve connects, using a cubic spline function, the average values of experimental points from intact fibers in *A*. Additional information on cut fibers is given in Table I. In this and other figures, except where noted, measurements of absorbance have been corrected for the intrinsic contribution (see Methods).

### *Resting Spectrum of Arsenazo III Inside Intact and Cut Muscle Fibers*

In any study with Ca indicators, it is important to compare the spectral properties of indicator inside a cell with those in a cuvette. The resting absorbance spectrum of arsenazo III inside intact muscle fibers was first measured by Baylor et al. (1982*a*) and Miledi et al. (1982). We repeated such measurements and the large symbols in Fig. 3*A* show results from three intact muscle fibers. The absorbance

data have been corrected for the intrinsic contribution. They have also been normalized by values of absorbance at 570 nm, the isosbestic wavelength for Mg and pH (as well as Ca), to compensate for changes in the indicator concentration. The small dots connected by a continuous curve represent cuvette calibration measurements made with pH 6.9 and a free [Mg] of 1.08 mM; for comparison, the internal solution for cut fibers had a pH of 7.0 and a free [Mg] calculated to be 1 mM. The cuvette curve in Fig. 3*A* is in fair but not perfect agreement with the fiber experimental points. The data between 520 and 560 nm lie slightly below the curve; those between 580 and 620 nm lie above it. The discrepancy is not surprising, since most of the indicator inside a fiber appears to be bound (column 5 of Table II or columns 3 and 6 of Table III) and bound indicator may well have an absorbance different from that of free indicator.

Fig. 3*B* shows the absorbance spectrum of arsenazo III inside three cut fibers. The continuous curve gives the average value of the intact fiber measurements in Fig. 3*A*. There is good agreement between the points and the curve, at least for $\lambda \geq 500$ nm, where the intrinsic correction is not as critical as at shorter wavelengths. Thus, arsenazo III has the same absorbance spectrum inside either cut or intact fibers.

The effect on the resting spectrum of either the experiment duration or the indicator concentration was not systematically investigated. The ratio $A(660)/A(570)$ showed little variation during experiments and no consistent change with either the experiment duration or the indicator concentration.

We also looked for the presence of resting dichroism such as might arise from oriented arsenazo III molecules. Since $A(570, \delta)$ and $A(750, \delta)$ are approximately equal in a cut fiber without an indicator (unpublished observations), the difference $A(570, \delta) - A(750, \delta)$ was used to estimate arsenazo III–related dichroism. Data from five fibers were analyzed. In these fibers, arsenazo III–related dichroism was positive and increased with the arsenazo III–related $A(570, 1{:}2)$ or the indicator concentration in an approximately linear manner. The ratio [arsenazo III–related dichroism]:[arsenazo III–related $A(570, 1{:}2)$] varied from 0.030 to 0.057, with an average value of 0.043 (SEM = 0.004); this is significantly different from 0 at the level $P < 0.005$ using the two-tailed $t$ test. Thus, arsenazo III–related dichroism is present but small in magnitude. It is probably due to oriented indicator molecules.

### *Absorbance Changes after Action Potential Stimulation in Fibers Containing Arsenazo III*

Fig. 4*A* shows absorbance changes associated with a single action potential in a cut fiber containing arsenazo III, mode 1 recording (Fig. 3 in Irving et al., 1987). The top trace shows the action potential. Its waveform has been heavily attenuated by the 0.625-kHz Bessel filter; the actual peak amplitude, measured with a storage oscilloscope, was 134 mV. The next six records show absorbance changes for light of three different wavelengths and two linear polarizations, oriented at 0° and 90° with respect to the fiber axis. As shown in Fig. 16 of Irving et al. (1987), the waveforms of the optical signals are not distorted by the Bessel filter; they are simply shifted 1.6 ms to the right.

The noise levels are different on the three pairs of optical traces in Fig. 4*A*. The 660-nm records are less noisy than the 750-nm records because half the total light was used for the 660-nm signal, whereas one-fourth was used for the 750-nm signal. The 750-nm records have less noise than the 570-nm records, also obtained with one-fourth the total light, for two reasons: the intensity of

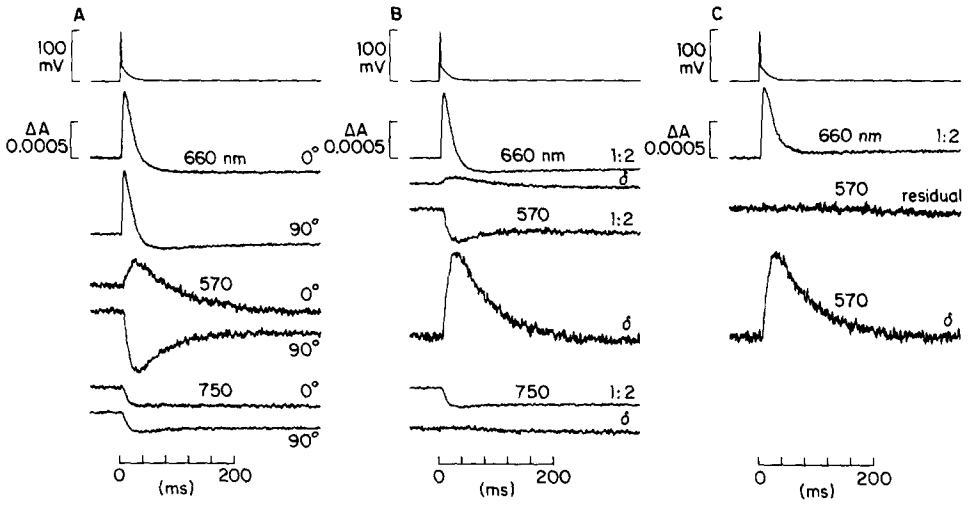


FIGURE 4. Optical changes that follow action potential stimulation in a cut fiber containing arsenazo III. (*A*) The top trace shows an action potential, attenuated by the 0.625-kHz eight-pole Bessel filter; the actual peak amplitude was 134 mV. The next traces show the six optical records, not corrected for intrinsic contributions, taken in mode 1, with the wavelength and direction of polarization indicated. In this and subsequent figures, the $t = 0$ marker indicates the moment, shifted by the low-frequency delay of the Bessel filters (equal to the reciprocal of the cutoff frequency), when electrical stimulation was initiated. The optical filters employed were 570 nm (10-nm bandpass) in the $\lambda_1$ position, 660 nm (30-nm bandpass) in $\lambda_2$, and 750 nm (30-nm bandpass) in $\lambda_3$ (Irving et al., 1987). (*B*) The raw absorbance changes in panel *A* have been combined to give 1:2 absorbance changes and dichroic absorbance changes, $\delta$. (*C*) The 570- and 660-nm optical signals in *B* have been corrected for the fiber's intrinsic signal, obtained at 750 nm, to give the arsenazo III–related absorbance changes $\Delta A(660, 1{:}2)$, or the Ca signal, and $\Delta A(570, \delta)$, or the dichroic signal. The correction is based on Eq. 2 with $n = 0.8$. The 570-nm residual trace is the difference between the $\Delta A(570, 1{:}2)$ trace in *B* and a best-fit linear combination of $\Delta A(570, \delta)$ and $\Delta A(750, 1{:}2)$ in *B*. The scaling constants were 1.237 for $\Delta A(750, 1{:}2)$ and $-0.104$ for $\Delta A(570, \delta)$. The nonzero value of the second constant indicates that the changes in 570-nm absorbance, using 0° and 90° light, cannot be explained solely by a change in the orientation of indicator molecules in a fiber with radial symmetry; either radial symmetry did not strictly hold or there was an additional component to the signal caused by a change in indicator absorbance or by an indicator-related movement artifact. Fiber 060684.2; relevant information is given in the legend to Fig. 3*B*; arsenazo III concentration, 0.214 mM; time after saponin treatment, 30 min. In subsequent figures, unless otherwise noted, the absorbance traces have had their intrinsic contributions subtracted.

light from the tungsten-halogen bulb was greater at 750 nm than at 570 nm, and the 750-nm interference filter (and the 660-nm filter) had a 30-nm bandpass, whereas the 570-nm filter had a 10-nm bandpass.

Since 750-nm light is not absorbed by arsenazo III, the $\Delta A(750)$ records give the intrinsic signal (Fig. 4*A*). The 0° and 90° traces are nearly identical; they show a small early decrease in absorbance that was maintained for the duration of the sweep. This intrinsic signal is similar to that obtained from cut fibers that did not contain an indicator (Irving et al., 1987). It is also similar to that in intact fibers without an indicator, except that the early brief increase in absorbance (Baylor et al., 1982*a*) was less pronounced in cut fibers.

The 660-nm records in Fig. 4*A* show an early increase in absorbance caused by the formation of a Ca:arsenazo III complex. This Ca component was not maintained, and at later times the 660-nm records resembled those at 750 nm. The 0° and 90° traces are similar.

The two 570-nm records in Fig. 4*A*, in contrast to the other two pairs, are clearly different from one another. The early absorbance change peaked slightly later than the 660-nm Ca signal, and the 0° and 90° components were of opposite sign, which indicates substantial dichroism. At late times, both 570-nm signals reached a negative maintained level similar to that at 750 nm.

The optical traces in Fig. 4*A* are similar to those recorded from intact fibers injected with arsenazo III (Baylor et al., 1982*c*). They consist of three basic components: an intrinsic signal (easily resolved at 750 nm, where there are no indicator-related signals), a Ca signal (near maximum at 660 nm, where there is little dichroic contribution), and a dichroic signal (near maximum at 570 nm, where there is little Ca contribution).

Fig. 4*B* shows linear combinations of the records in *A*. The label "1:2" denotes $(\Delta A_0 + 2\Delta A_{90})/3$. In a cell with radial symmetry, changes in the orientation of indicator molecules should make no contribution to this average (Baylor et al., 1982*c*). The $\Delta A(660, 1{:}2)$ and $\Delta A(750, 1{:}2)$ signals are similar to the respective original records in panel *A*, as expected since the 0° and 90° records were almost the same. Although the 570-nm 0° and 90° records were quite different, the $\Delta A(570, 1{:}2)$ signal resembles $\Delta A(750, 1{:}2)$. This similarity has also been found in intact fibers; there the changes in 0° and 90° 570-nm absorbance have been shown to arise primarily from a change in the orientation of arsenazo III molecules (Baylor et al., 1982*c*), which, as mentioned above, does not contribute to a 1:2 average.

The other combination of records in Fig. 4*B* is labeled "$\delta$"; this represents $\Delta A_0 - \Delta A_{90}$ and is called the dichroic signal. It is nearly flat at 750 nm, small at 660 nm, and relatively large at 570 nm. Since the intrinsic 750-nm signal is small, almost all the signal at 570 and 660 nm can be attributed to the presence of arsenazo III; consequently, there is little need to correct the dichroic traces at these wavelengths for changes in intrinsic fiber dichroism.

The 660- and 570-nm 1:2 signals, on the other hand, have a significant intrinsic component. Since both the amplitude and wavelength dependence of this component can change during the time course of a cut fiber experiment (Irving et al., 1987), it was important to have a method for estimating both from

signals taken in the presence of arsenazo III. The $\Delta A(570, 1{:}2)$ signal was assumed to consist of two components, an intrinsic component that has the same waveform as $\Delta A(750, 1{:}2)$ and a second component that has the $\Delta A(570, \delta)$ waveform. A linear combination of these two basic waveforms was fitted to $\Delta A(570, 1{:}2)$ using a least-squares computer program. The trace in Fig. 4*C* labeled "570 residual" shows the difference between $\Delta A(570, 1{:}2)$ and the fitted linear combination; the fit is good, as evidenced by the flatness of the residual. Next, the wavelength dependence of the intrinsic signal, the power $n$ in Eq. 2, was determined from the scaling constant for $\Delta A(750, 1{:}2)$, 1.237 in this case, which gave $n = 0.8$. The 750-nm traces in Fig. 4*B* were then scaled using Eq. 2 and $n = 0.8$ to give estimates of the intrinsic contributions to the 660- and 570-nm traces. This procedure for estimating the intrinsic contributions worked well in fibers that did not contain any indicator.

The estimated intrinsic components were subtracted from the traces in Fig. 4*B* to give indicator-related signals, two of which are shown in Fig. 4*C*. The $\Delta A(660, 1{:}2)$ signal provides the best estimate we have of the Ca-related absorbance change of arsenazo III. The signal does not decay to baseline at late times, however, possibly because of maintained changes in [Ca], pH, or [Mg] (Baylor et al., 1982*b*) or an error in the estimate of the intrinsic contribution. The $\Delta A(570, \delta)$ signal, which required only a minor intrinsic correction, represents the arsenazo III–related dichroic signal. In the rest of this article, unless noted otherwise, absorbance signals have been corrected for intrinsic contributions. The corrected $\Delta A(660, 1{:}2)$ is frequently called the Ca signal and the corrected $\Delta A(570, \delta)$ is called the dichroic signal.

### *Effect of Arsenazo III Concentration and Duration of Experiment on the Ca and Dichroic Signals*

Fig. 5*A* shows the time course of arsenazo III concentration during the experiment used for Fig. 4. The curve was calculated from Eqs. 6 and 8 using the best-fit parameters given in Table II. Panels *B* and *C* show, respectively, Ca and dichroic signals elicited by action potential stimulation. The identification letters *a*–*d* refer to experimental points in Figs. 5 and 6; the traces labeled *b* are the same as those in Fig. 4*C*.

The absorbance traces in Fig. 5, *B* and *C*, have been corrected for intrinsic contributions using the procedure described in Fig. 4. During the experiment, the parameter $n$ in Eq. 2 varied from 0.1 for trace *a* to 2.1 for *d*. Variations in $n$ have also been observed in fibers that did not contain an indicator (Figs. 13 and 14 in Irving et al., 1987). The variation in those experiments was less than in Fig. 5 but the period of observation was shorter. Nevertheless, the wavelength of the intrinsic signal, 750 nm, is close to that of the Ca signal, 660 nm, and the intrinsic dichroic signal is small, so that the intrinsic corrections do not depend critically on the exact value used for $n$.

As indicator diffused into the fiber in Fig. 5, the peak amplitude of the Ca signal increased from *a* to *b* to *c* (panel *B*). Then, as indicator diffused out, the amplitude decreased from *c* to *d*. The concentration of indicator was about the same in *b* and *d*, so that one might expect the two $\Delta A(660, 1{:}2)$ signals to be the

same. The peak amplitudes of the two signals were indeed similar but the durations were different, being longer in *d* than in *b*. The dichroic signals in *C* also changed during the experiment but in a different manner. At *a*, the dichroic

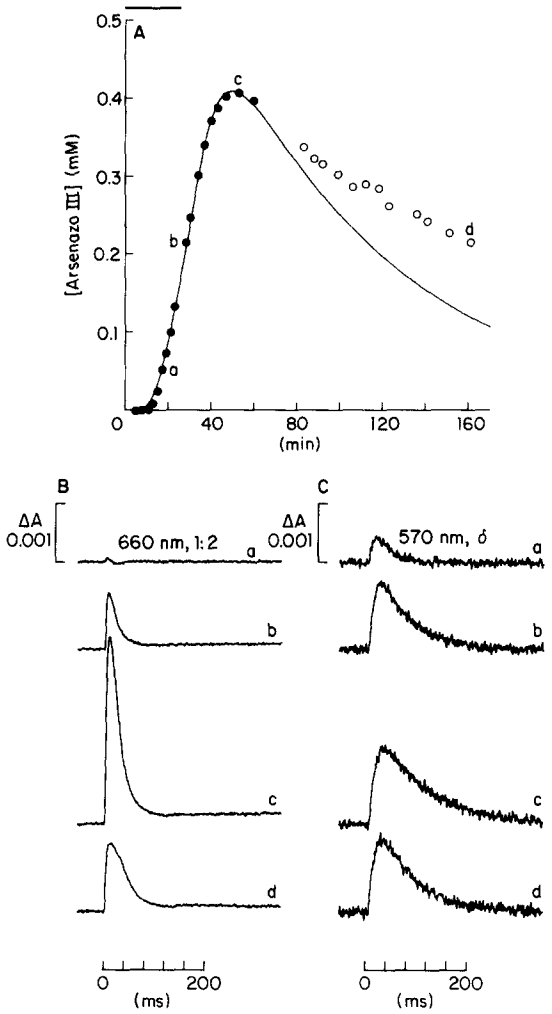


FIGURE 5. Optical signals recorded with different internal concentrations of arsenazo III. (*A*) Arsenazo III concentration plotted against time after the addition of 0.5 mM indicator to the end pools 2 min after saponin treatment. The duration of arsenazo III exposure, 26 min, is indicated by the horizontal bar. The continuous curve shows a least-squares fit of Eqs. 6 and 8 to the filled symbols, using the parameters given in columns 4 and 5 of Table II. (*B* and *C*) Traces of $\Delta A(660, 1{:}2)$ and $\Delta A(570, \delta)$, respectively, taken at different times. The intrinsic correction used Eq. 2 with $n = 0.1$ (*a*), 0.8 (*b*), 1.4 (*c*), and 2.1 (*d*). The identification letters *a–d* reference experimental points and traces in this figure and in Fig. 6. Same experiment as in Fig. 4.

trace was pronounced, whereas the Ca trace was almost flat. In *b*, *c*, and *d*, the amplitude of the dichroic signal was nearly constant, whereas that of the Ca trace showed considerable variation.

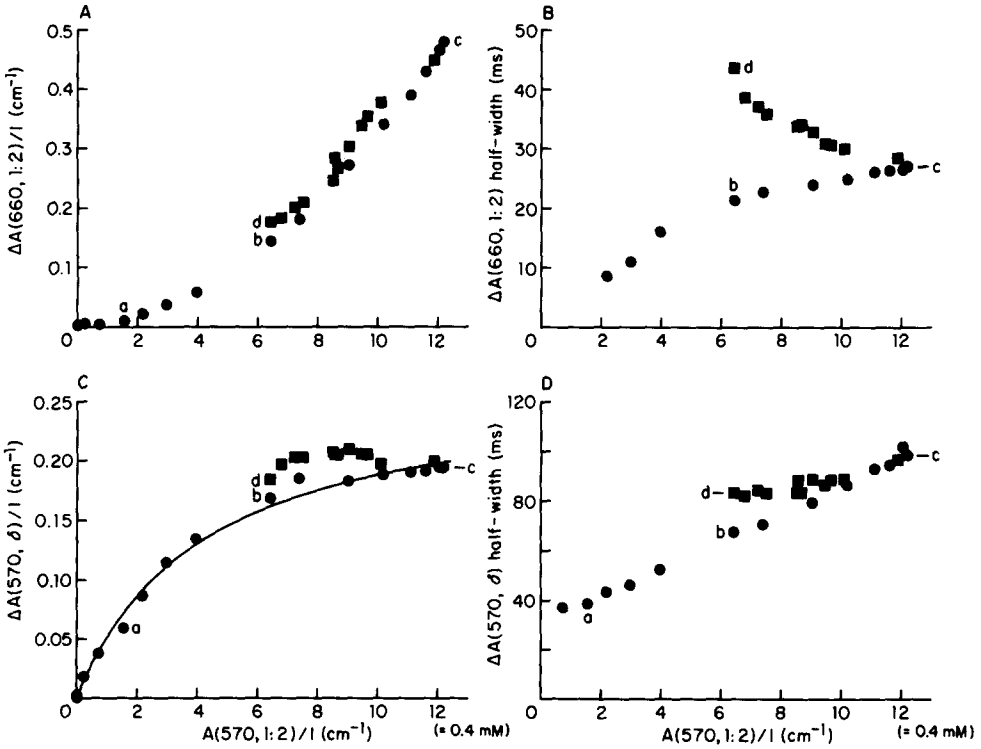


FIGURE 6. Effect of arsenazo III concentration on the magnitude and half-width of the Ca and dichroic signals. (*A* and *B*) Peak amplitude and half-width, respectively, of $\Delta A(660, 1{:}2)/l$ plotted against resting $A(570, 1{:}2)/l$, or the indicator concentration. The half-width is defined as the interval that elapsed between the time to half-peak on the rising phase and the time to half-peak on the falling phase. The measurements indicated by the circles and squares were made, respectively, as the arsenazo III concentration was increasing and decreasing with time. (*C* and *D*) Peak amplitude and half-width, respectively, of $\Delta A(570, \delta)/l$ plotted against resting $A(570, 1{:}2)/l$; the symbols have the same meaning as in *A* and *B*. The continuous curve in *C* shows a least-squares fit of Eq. 12 to the points shown as circles, with $K_D$ = 4.2/cm (which corresponds to an indicator concentration of 0.14 mM) and a maximum value of 0.27/cm. Same experiment as shown in Fig. 5; the traces associated with experimental points *a–d* are shown in Fig. 5, *B* and *C*.

Fig. 6 considers the effect of indicator concentration on the Ca and dichroic signals in this experiment in more detail. Panel *A* shows the relation between peak $\Delta A(660, 1{:}2)/l$ and $A(570, 1{:}2)/l$, which, according to Eq. 3, is proportional to the indicator concentration. Absorbance measurements have been normalized by path length $l$ to correct for any changes in fiber diameter; in this experiment,

the diameter was 98 μm at the beginning of the experiment and 94 μm at the end (Table I, column 4). The experimental points in Fig. 6*A* show an approximately parabolic relation between the amplitude of the Ca signal and the internal indicator concentration. The same relation appeared to hold whether the arsenazo III concentration was increasing (circles) or decreasing (squares). This shape would be consistent with a 1:2 or 2:2 stoichiometry for the Ca:indicator complex, as suggested by Thomas (1979), Palade and Vergara (1981, 1983), and Rios and Schneider (1981). It could also be consistent with a 1:1 stoichiometry if the first indicator molecules to reach the optical site were bound or sequestered and unable to react with Ca; such binding might be responsible for the dichroic signal, as discussed below. In light of these and other uncertainties about arsenazo III (Baylor et al., 1983*b*; Quinta-Ferreira et al., 1984), no attempt was made to fit a calibration curve to the data in Fig. 6*A*.

Fig. 6*B* shows the half-width of the Ca signal plotted against the arsenazo III concentration. As arsenazo III diffused into the fiber, the half-width increased (points *b* and *c*; the half-width of trace *a* could not be determined). It continued to increase as arsenazo III diffused out of the fiber (from *c* to *d*). The relation between the half-width and the concentration was not single-valued. Instead, the half-width increased monotonically during the entire experimental period. This argues against a reversible effect of the indicator on the half-width such as might be produced, for example, by buffering Ca. Such an increase is not peculiar to arsenazo III; it also occurs with antipyrylazo III Ca signals (Maylie et al., 1987) and with retardation signals in fibers without indicator (Fig. 15 in Irving et al., 1987).

The prolongation of the Ca waveform occurred with little change in either the relation between peak $\Delta A(660)$ and indicator concentration (Fig. 6*A*) or in the time course of the rising phase of the Ca signal. The time to half-peak of the signal, following that of the action potential, was 4.08 ms in *b* and 4.17 ms in *d*; in *c*, the time to half-peak was somewhat longer, 4.52 ms, owing to a small, reversible effect of indicator concentration. There was also no obvious deterioration in the electrical condition of the fiber (fiber 060684.2 in Table I). At the beginning of the experiment, the peak amplitude of the action potential was 132 mV; it then climbed to 134 mV and finally returned to 132 mV by the end of the experiment. The holding current was initially −75 nA; it remained almost constant throughout the experiment and was −74 nA at the end. The value of $r_m$ declined from 0.088 MΩ·cm at the beginning of the experiment to 0.077 MΩ·cm at the end. The variation in $r_e/(r_e + r_i)$ was slight, from 0.966 to 0.963.

Fig. 6*C* shows the amplitude of the dichroic signal plotted against the arsenazo III concentration. The relation is different from that shown for the Ca signal in *A*. The dichroic data obtained during indicator entry (circles) were fitted by the 1:1 binding isotherm:

$$y = y_{max} \cdot \frac{A(570,\ 1{:}2)/l}{A(570,\ 1{:}2)/l + K_D}, \tag{12}$$

in which $y$ represents peak $\Delta A(570, \delta)/l$. The continuous curve shows the fit with $K_D = 4.2$/cm (in units of absorbance per unit path length), which corresponds to an arsenazo III concentration of 0.14 mM.

Table IV gives values of $y_{max}$ and $K_D$ obtained by fitting Eq. 12 to data from four experiments. On average, $K_D = 0.117$ mM and $y_{max} = 0.24$/cm. The average cut fiber curve can be compared with the concentration dependence in intact fibers shown in Fig. 9 of Baylor et al. (1982*c*). Since the measurements of absorbance in intact fibers were not corrected for the path length factor 0.7 (see Methods), the cut fiber values of $K_D$ and $y_{max}$ should be multiplied by 0.7 for the purpose of comparison. The resulting curve, determined with $K_D = 0.08$ mM and $y_{max} = 0.17$/cm, lies within the upper range of the data from intact fibers.

Fig. 6*D* shows the half-width of the dichroic signal plotted against the arsenazo III concentration. The half-width increased from ~40 to ~100 ms as the indicator concentration increased (circles, *a–c*). Then, as the indicator concentration decreased (squares, *c–d*), the half-width decreased and remained approximately constant. The half-widths of both the Ca and the dichroic signal were greater at *d* than *b*, a finding that is qualitatively consistent with the mechanism of the dichroic signal suggested by Baylor et al. (1982*c*). According to their scheme, Ca

TABLE IV

*Effect of Indicator Concentration on the Arsenazo III Dichroic Signal*

| (1) Fiber reference | (2) $y_{max}$ | (3) $K_D$ | (4) $K_D$ |
|---|---|---|---|
| | $cm^{-1}$ | $cm^{-1}$ | *mM* |
| 060684.1 | 0.22 | 2.8 | 0.093 |
| 060684.2 | 0.27 | 4.2 | 0.140 |
| 060784.2 | 0.16 | 3.4 | 0.113 |
| 100184.1 | 0.30 | 3.6 | 0.120 |
| Mean | 0.24 | 3.5 | 0.117 |
| SEM | 0.03 | 0.3 | 0.010 |

Column 1 gives fiber reference. Columns 2 and 3 give the values of the parameters (in units of absorbance per unit path length) in Eq. 12 that gave a least-squares fit. Column 4 gives $K_D$ in units of millimolar. Fiber information is given in Table I.

binds to high-affinity sites on oriented myoplasmic structures, such as thin filaments or sarcoplasmic reticulum, and this produces a change in the orientation of arsenazo III molecules that are associated with or bound to the same structure but are not necessarily near the Ca-binding site. To take this idea further requires a reliable estimate of the free [Ca] waveform, and this is difficult to obtain with arsenazo III (Baylor et al., 1983*b*; Quinta-Ferreira et al., 1984).

The half-width of the dichroic signal was monitored in two other pulsed-exposure experiments. In both fibers, it increased as the indicator concentration increased and, in contrast to the results in Fig. 6*D*, continued to increase as the concentration decreased. The irreversible increase in the half-width of the dichroic signal was more marked in these two fibers than in the one in Fig. 6.

The concentration of arsenazo III in the fiber in Figs. 4–6 never exceeded 0.4 mM. This low range of concentrations was chosen to minimize the buffering action of the indicator and consequent perturbation of the free [Ca] transient. In contrast, Fig. 7 shows an experiment in which 1 mM arsenazo III was in the end pools for >3 h and the concentration at the optical recording site reached almost 3 mM. Panel *A* shows the time course of indicator concentration and the

theoretical fit of Eqs. 6 and 8. The value of $(R + 1)$ in this experiment was 3.536; this is similar to the values obtained in Fig. 1, *A* and *B*, 3.469 and 3.551, in which only half the concentration of arsenazo III was used, and similar to the average value obtained from all fibers, 3.717 (Table II, column 5).

Fig. 7*B* shows an action potential and four representative Ca signals. As arsenazo III diffused into the fiber, both the amplitude and the duration of the

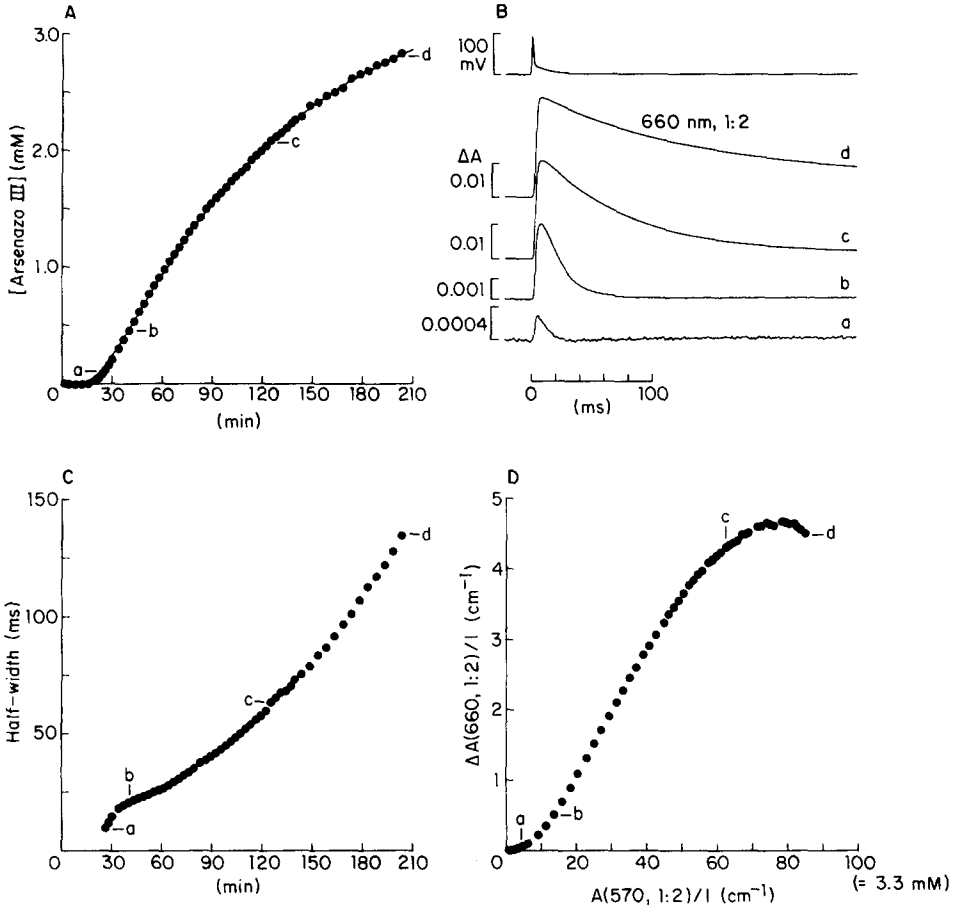


FIGURE 7. Changes in the Ca signal during a long exposure to arsenazo III. (*A*) Arsenazo III concentration plotted against time after the addition of 1 mM indicator to the two end pools 19 min after saponin treatment. The continuous curve is a least-squares fit of Eqs. 6 and 8 using the parameters given in Table II. (*B*) Single record of an action potential and four traces of $\Delta A(660, 1{:}2)$ taken at different times. Intrinsic corrections were made with Eq. 2 and $n = 0.2$. (*C*) Half-width of $\Delta A(660, 1{:}2)$ plotted against time. (*D*) Peak amplitude of $\Delta A(660, 1{:}2)/l$ plotted against $A(570, 1{:}2)/l$, or indicator concentration. Fiber 100184.1; sarcomere spacing, 3.7 μm. In this and the next two figures, the letters *a–d* have been used to identify experimental points in panels *A*, *C*, and *D* with individual traces in panel *B* of the same figure.

Ca signal increased. The half-width of the Ca signal increased from 9.8 to 135 ms (*C*) with little change in the parameters used to monitor fiber viability (Table I, fiber 100184.1). The peak amplitude (*D*) had a roughly parabolic dependence on arsenazo III concentration at low concentrations, similar to that shown in Fig. 6*A*, but showed saturation at high concentrations.

*Amplitude and Half-Width of Ca Signals in Intact and Cut Fibers*

Arsenazo III Ca signals in cut fibers are similar to those in intact fibers. Fig. 5 in Miledi et al. (1982) illustrates an experiment in which arsenazo III was slowly injected into an intact muscle fiber that was periodically stimulated to produce action potentials. The amplitude of the Ca signal increased as the indicator entered the fiber. The relation between the peak $\Delta A$ and the indicator concentration was linear between 0.2 and 1 mM, with an extrapolated intercept on the concentration axis at ~0.1 mM. The rate of decay of the Ca signal was nearly constant until the arsenazo III concentration reached 0.5 mM; thereafter, it became progressively slower as the concentration increased further.

Figs. 3 and 4 in Baylor et al. (1982*b*) show results from intact fibers in which a different protocol was followed. Arsenazo III was quickly injected into a fiber. Then optical signals were periodically recorded as the indicator concentration decreased as a result of diffusion along the fiber. In these experiments, the duration of the Ca signal decreased with time and its amplitude varied with the arsenazo III concentration in an approximately linear manner, with an extrapolated intercept near 0 mM.

Thus, in intact fibers, the amplitude of the Ca signal varies with the arsenazo III concentration in an approximately linear manner, with an extrapolated intercept on the concentration axis between 0 and 0.1 mM. This concentration dependence is qualitatively similar to that shown for cut fibers in Figs. 6*A* and 7*D*.

In intact fibers, the duration of the Ca signal shows a monotonic increase with arsenazo III concentration, during periods when the indicator concentration either increases with time (Miledi et al., 1982) or decreases (Baylor et al., 1982*b*). In cut fibers, however, the duration can change in a different way. The increase in half-width shown in Fig. 7*C* is much greater than any reported in intact fibers. In Fig. 6*B*, the large increase in half-width from *c* to *d*, when the indicator concentration was decreasing, is also in marked contrast to intact fiber results. This suggests that the physiological state of cut fibers may change with time in a way that does not happen in intact fibers.

To test this idea further, we measured Ca signals in intact and cut fibers under closely similar conditions. Fig. 8 shows an experiment in which arsenazo III was injected into a singly dissected intact fiber. Panel *A* gives the time course of the indicator concentration after a 2.5-min injection, which ended at $t = 0$, near the site of optical recording; the exact distance between the injection and recording sites was not noted but was probably 50–150 $\mu$m. The theoretical curve was calculated from $(t + 1.25 \text{ min})^{-1/2}$ and scaled, arbitrarily, to fit the experimental point at $t = 20$ min. A $(t + 1.25 \text{ min})^{-1/2}$ relation would be expected from Eqs. 5 and 8 if all the indicator were injected at the recording site at $t = -1.25$ min. This idealized initial condition does not work well at very early times but

introduces little error by 10–20 min, after which the experimental points and theoretical curve can be directly compared. In this experiment, the theoretical curve fitted the experimental points reasonably well. Two other experiments showed slight discrepancies, in the same direction as that in Fig. 9*A*, but the

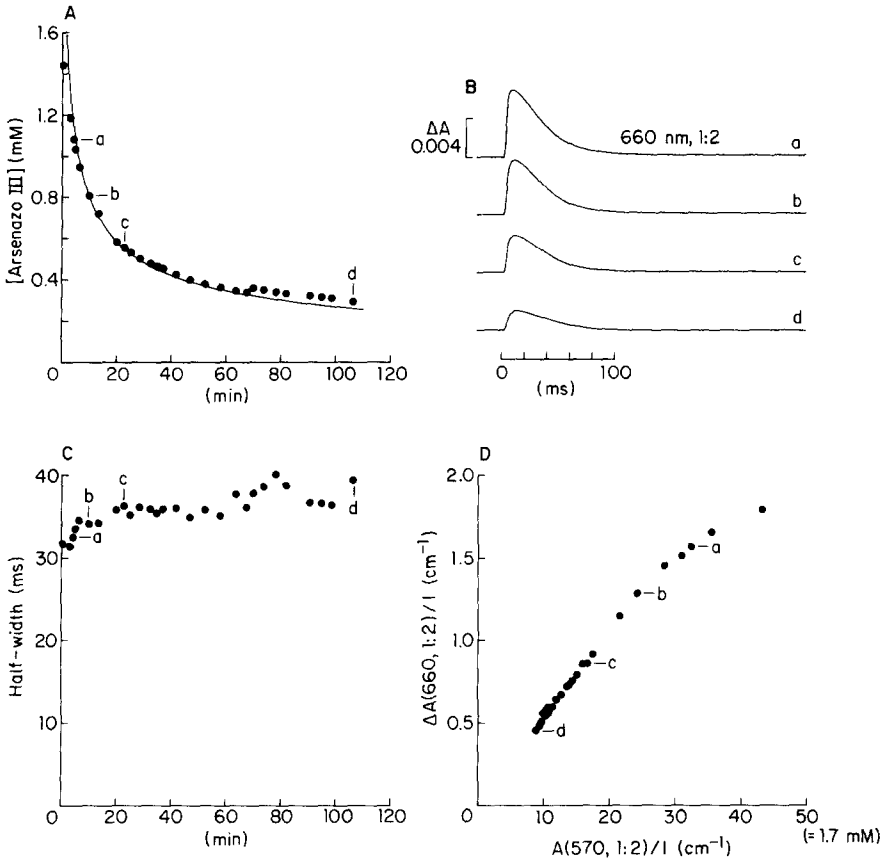


FIGURE 8. Properties of arsenazo III Ca signals in an injected intact fiber. (*A*) Concentration of arsenazo III plotted against time after the end of a 2.5-min injection by microelectrode. The continuous curve was calculated from $(t + 1.25 \text{ min})^{-1/2}$ and scaled to fit the experimental point at 20 min. (*B*) Four traces of $\Delta A(660, 1{:}2)$ elicited by action potential stimulation at different times; $n = 4$ was used for the intrinsic correction (Eq. 2). (*C*) Half-width of $\Delta A(660, 1{:}2)$ plotted against time. (*D*) Peak amplitude of $\Delta A(660, 1{:}2)/l$ plotted against $A(570, 1{:}2)/l$, or indicator concentration. Fiber 041583.2; diameter, 63 μm; sarcomere spacing, 4.0 μm; Ringer's solution; temperature, 15.8–16.2°C.

studies were terminated too early for us to be certain. Thus, additional experiments would be required to decide whether the agreement in Fig. 8*A* is typical of results from intact fibers.

Fig. 8*B* shows Ca signals recorded at various times after injection. The half-

width increased slightly during the experiment (Fig. 8*C*); this slight increase is somewhat different from the slight decrease previously found in intact fibers injected and studied the same way (Baylor et al., 1982*b*). Panel *D* shows the peak amplitude of the Ca signal plotted against the arsenazo III concentration. At concentrations <0.7 mM, the relation is linear and extrapolates through the origin, similar to the intact fiber in Fig. 4*A* of Baylor et al. (1982*b*). In two other experiments on intact fibers, the decrease in the indicator concentration was less marked, and the extrapolated intercept on the concentration axis, probably 0.1–0.2 mM, was less certain (Fig. 10*A*, dashed lines).

The experimental protocol in Fig. 8 was repeated on a saponin-treated cut fiber injected with arsenazo III. Fig. 9 gives the results, arranged in the same format as Fig. 8. Panel *A* shows the time course of indicator concentration and a theoretical curve similar to that in Fig. 8*A*. The experimental points are well above the curve at late times, which indicates that Eqs. 5 and 8 do not describe the diffusion and binding of arsenazo III in this experiment; a similar discrepancy was found in two other experiments on cut fibers.

Fig. 9*C* shows the variation in the half-width of the Ca signal as arsenazo III diffused away from the injection site. From *a* to *b*, the half-width decreased. A similar decrease has been observed in intact fibers (Miledi et al., 1982; Baylor et al., 1982*b*) and may be related to the decreasing indicator concentration (*A*). From *b* to *c* to *d*, the half-width increased. This relatively large change was not observed in Fig. 8*C* or in any other experiment on intact fibers.

Fig. 9*D* shows the concentration dependence of the amplitude of the Ca signal. The relation is qualitatively similar to that in Fig. 8*D*. The bend between points *c* and *d* in Fig. 9*D* was peculiar to this experiment and was not seen in two other injected cut fibers. In those fibers, the relation between the Ca signal amplitude and the arsenazo III concentration was approximately linear at late times, with an extrapolated intersection on the concentration axis at 0.1–0.2 mM, which is similar to the experiments on intact fibers in this article and in Miledi et al. (1982). The exact location of the intercept on the concentration axis depends heavily on the experimental points associated with the smallest concentrations of indicator. In our experiments on injected fibers, such points were taken at late times and are therefore sensitive to any long-term changes in fiber condition (Fig. 9*D*, for example). Consequently, we are reluctant to attach much significance to variations in the value of this intercept in the range 0–0.2 mM.

Fig. 10 shows a summary of amplitude and half-width information for arsenazo III Ca signals recorded from injected twitch fibers prepared three different ways: intact (dashed lines), cut and treated with saponin (continuous lines), and cut but not treated with saponin (dotted lines). The cut fibers not treated with saponin had 1–2-mm segments in the end-pool regions; consequently, the diffusion path length between the optical recording site and the end-pool solution was considerably greater in these fibers than in those treated with saponin. Panel *A* shows the amplitude of the Ca signal plotted against the indicator concentration. The relation appears to be the same in the various preparations. Panels *B* and *C* show the half-width of the Ca signal plotted against indicator concentration and time, respectively. In two of the three cut fibers treated with saponin (continuous line segments), the increase in half-width at late times was considerably more marked

than any changes seen in either intact or non–saponin-treated cut fibers (*C*). This difference suggests that the increase in half-width is not simply a result of the procedure for preparing and mounting cut fibers but requires making the membrane in the end pools permeable. A similar increase in the half-width was observed when notches were cut in the end-pool segments (see Fig. 6*C* in Maylie et al., 1987).

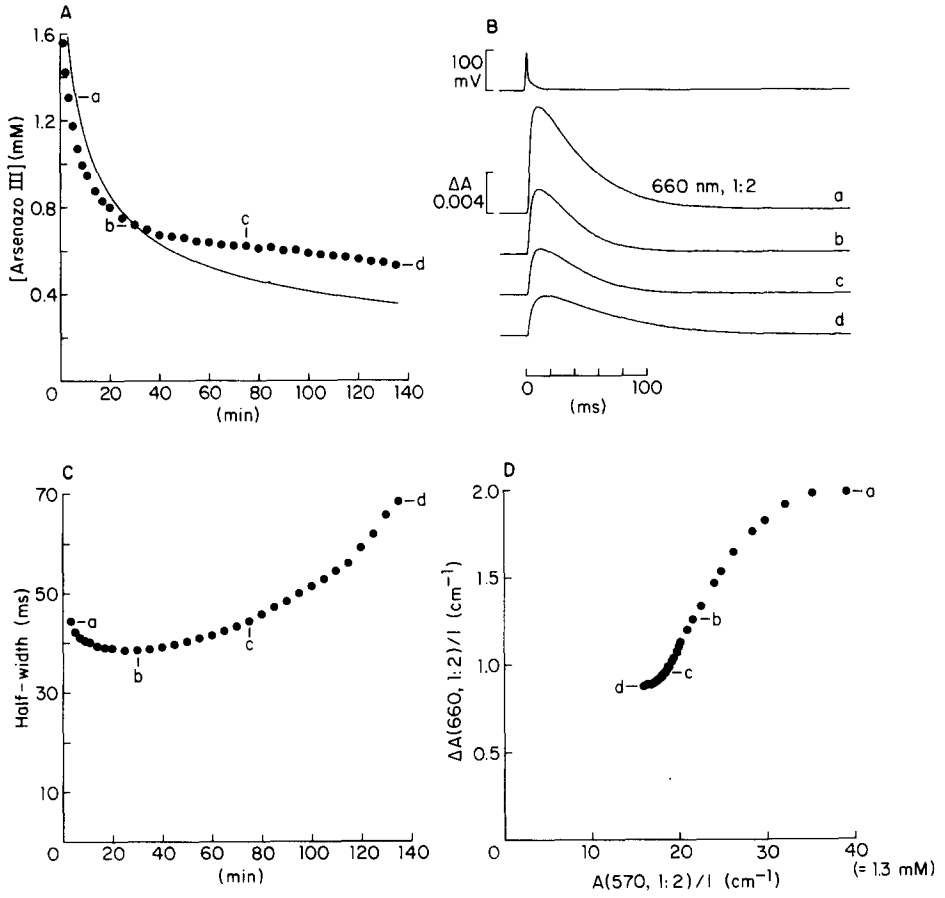


FIGURE 9. Properties of Ca signals after injection of arsenazo III into a saponin-treated cut fiber. (*A*) Concentration of arsenazo III plotted against time after the end of an 8-min injection by microelectrode; the injection was started 43 min after saponin treatment. The point of impalement was 50 μm in the direction of the fiber axis away from the edge of the site of optical recording. The continuous curve was calculated from $(t + 4 \text{ min})^{-1/2}$ and scaled to fit the experimental point marked *b*. (*B*) Single action potential record and four traces of $\Delta A(660, 1{:}2)$ taken at different times; the intrinsic correction used Eq. 2 and $n = 2.3$. (*C*) Half-width of $\Delta A(660, 1{:}2)$ plotted against time. (*D*) Peak amplitude of $\Delta A(660, 1{:}2)/l$ plotted against $A(570, 1{:}2)/l$, or indicator concentration. Fiber 092884.1; sarcomere spacing, 4.1 μm. Additional information about the fiber is given in Table I.

*Summary of the Effect of Arsenazo III Concentration on the Amplitude and Half-Width of Ca Signals in Saponin-treated Cut Fibers*

Because it is possible that arsenazo III introduced into cut fibers by injection behaves differently from that introduced by diffusion from cut ends, we com-

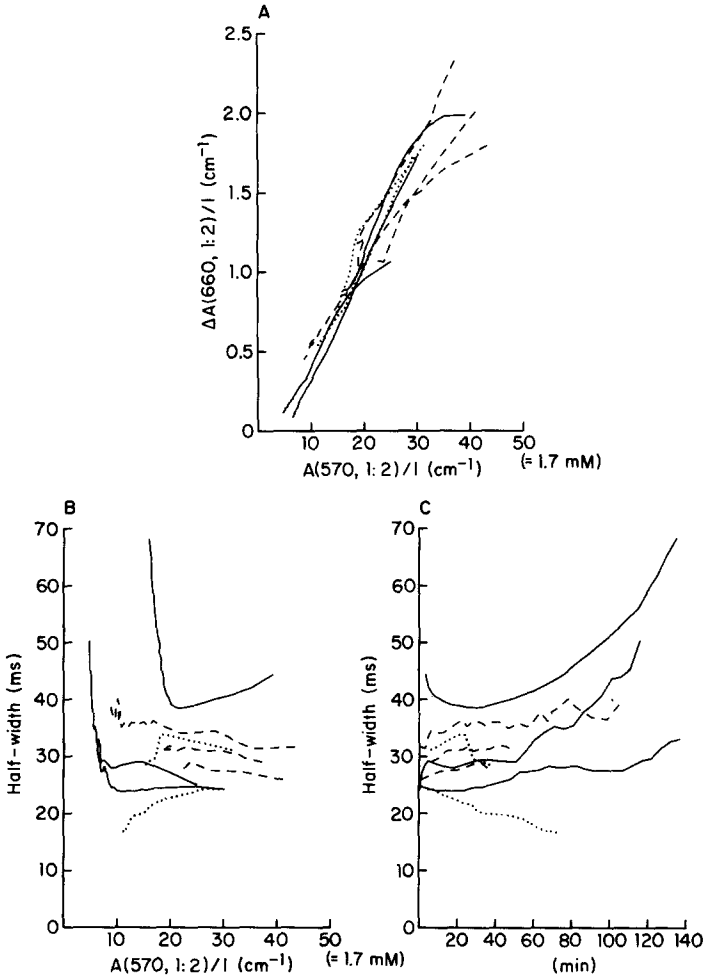


FIGURE 10. Comparison of peak amplitude and half-width of Ca signals after injection of arsenazo III into intact fibers and cut fibers with and without saponin treatment. (*A*) Peak amplitude of $\Delta A(660, 1{:}2)/l$ plotted against $A(570, 1{:}2)/l$, or indicator concentration. (*B* and *C*) Half-width of $\Delta A(660, 1{:}2)$ plotted, respectively, against $A(570, 1{:}2)/l$ and time after the end of the injection. The dashed line segments connect experimental points from intact fibers; the dotted line segments connect points from cut fibers that were not treated with saponin and had 1–2-mm lengths of fiber in the end-pool regions; the continuous line segments connect points from saponin-treated cut fibers in which the indicator injection was started 23–67 min after saponin treatment. The same protocol was used in all experiments. Diameter, 63–122 μm; sarcomere spacing, 3.7–4.2 μm; Ringer's solution; average temperature, 17.2°C.

pared results from injection and diffusion experiments. Fig. 11 shows the concentration dependence of the peak amplitude of the Ca signal in saponin-treated cut fibers studied with action potential stimulation. The continuous curves connect experimental points obtained as indicator diffused into five fibers and the dashed curves connect points from three injected fibers. Diffusion-introduced and injected arsenazo III produced Ca signals with similar amplitudes at similar indicator concentrations, which shows that the method of introduction does not influence the ability of the indicator to react rapidly with Ca.

It is difficult to compare the effect of arsenazo III concentration on the Ca signal half-width in diffusion-introduced and injected fibers. The results in Fig.

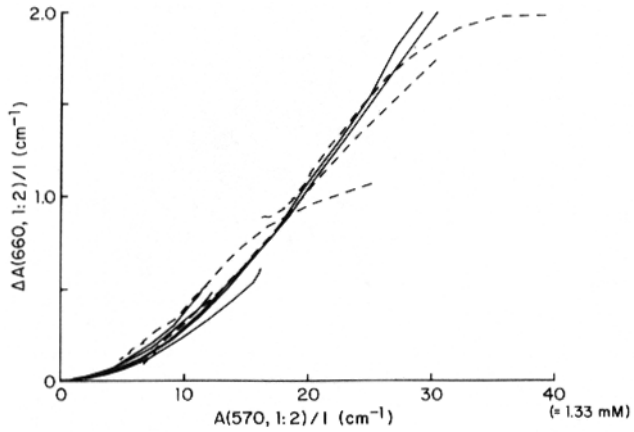


FIGURE 11. Comparison of peak amplitude of Ca signals in saponin-treated cut fibers into which arsenazo III was either injected or introduced by diffusion from the end pools. The peak amplitude of $\Delta A(660, 1{:}2)/l$ is plotted against $A(570, 1{:}2)/l$, or indicator concentration. The dashed line segments connect data points from injected fibers (same data as Fig. 10*A*, continuous lines); the continuous line segments connect data points from fibers into which arsenazo III diffused after addition to the end pools 2–29 min after saponin treatment (fibers 060684.1, 060684.2, 060784.2, 100184.1, and 100284.1 in Table I; fibers 070284.1, 070284.2, and 070284.3 could not be included since no more than two action potentials were elicited from each fiber once arsenazo III had entered). Fiber 100284.1 was studied in mode 2 so that the absorbance averages are 1:1 rather than 1:2.

6*B* show that the half-width increases continually with time in the presence of <0.4 mM indicator introduced by diffusion. The earliest Ca signal had a half-width of ~10 ms. Such a brief signal was never observed in an injected saponin-treated fiber (Fig. 10, *B* and *C*), perhaps because the concentration of indicator became low only at the end of an experiment, when the time-dependent increase in the half-width had become pronounced.

Fig. 12 shows the half-width of the Ca signal plotted against the arsenazo III concentration. The data were obtained early in experiments in which arsenazo III diffused into fibers. All five fibers showed a similar increase in half-width as arsenazo III first entered. At the lowest concentration at which the Ca signal

could be resolved, ~0.1 mM, the half-width was no more than 10 ms; at 0.3 mM, it had doubled. Some of this increase in half-width may be due to time-related changes in cut fibers. Most of it, however, is likely to be related to the use of arsenazo III since the increase observed with antipyrylazo III in a comparable period was much less marked (Fig. 10 in Maylie et al., 1987). Thus, arsenazo III appears to behave differently from antipyrylazo III.

Increasing the arsenazo III concentration may directly prolong the free [Ca] transient or may give a prolonged absorbance change in response to a constant, brief free [Ca] transient. Either possibility or a combination of the two is consistent with the results. One possible mechanism for a prolongation of the arsenazo III response is suggested by the findings of Quinta-Ferreira et al. (1984). They showed that the arsenazo III Ca signal can be described by a linear

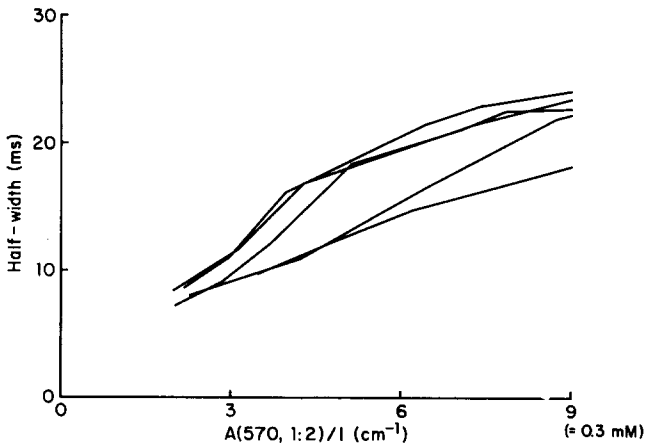


FIGURE 12. Half-width of Ca signals in saponin-treated cut fibers during the early phase of arsenazo III entry. Continuous line segments, connecting data points from the corresponding experiments in Fig. 11, are plotted against $A(570, 1{:}2)/l$ [$A(570, 1{:}1)/l$ in the case of fiber 100284.1], or indicator concentration. The indicator was added to the end pools 2–29 min after saponin treatment. Average temperature, 18.0°C.

combination of two waveforms, one that tracks free [Ca] rapidly and another that tracks [Ca] with a 10-ms delay. The results in Fig. 12 could be explained if the relative proportion of delayed to rapid waveforms increased with an increasing concentration of arsenazo III. This would be expected to happen if, for example, the rapid waveform were produced by the formation of a 1:1 Ca: indicator complex and the delayed waveform were produced by a 1:2 complex; the formation of a 1:1 complex would probably precede that of the 1:2 complex, and the proportion of the 1:2 to 1:1 complex should increase with increasing indicator concentration. This explanation is plausible since steady state cuvette calibrations suggest that both these complexes are present at the concentrations of Ca and arsenazo III employed here (Palade and Vergara, 1981, 1983; Rios and Schneider, 1981).

This tentative explanation illustrates the difficulty that can arise from the use of an indicator that can form more than one complex with Ca. Despite these difficulties, Fig. 12 clearly demonstrates that Ca signals in freshly prepared cut fibers measured with small concentrations of arsenazo III are extremely brief, with a half-width of <10 ms at 18°C.

*Wavelength Dependence of Active Arsenazo III Signals in Cut Fibers*

Fig. 13*A* shows changes in absorbance recorded at six different wavelengths after action potential stimulation. Each pair of traces shows absorbance changes

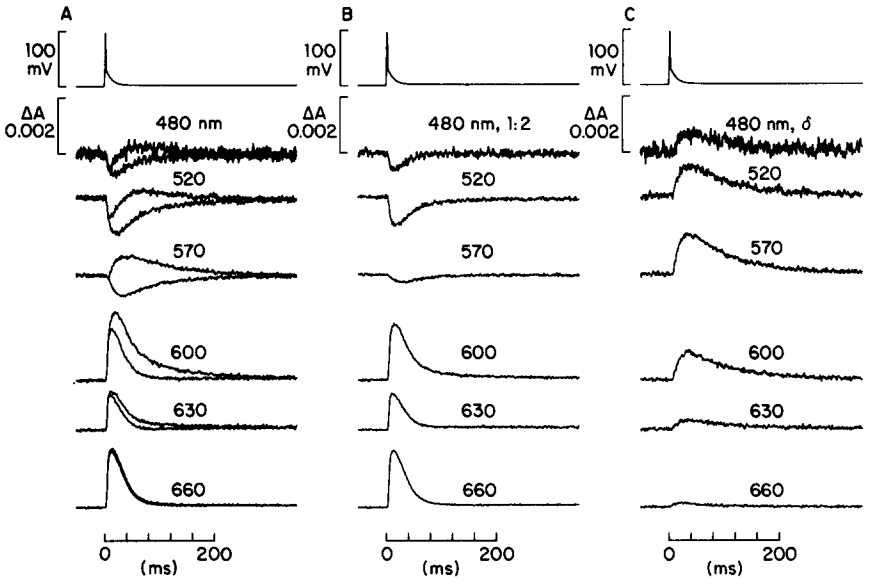


FIGURE 13. Changes in absorbance recorded at six wavelengths, mode 1. (*A*) Action potential record and six pairs of 0° and 90° absorbance traces; at each wavelength, the 0° trace is above the 90° trace. The 480–630-nm traces were obtained with 10-nm bandpass filters in the $\lambda_1$ position; the 660-nm traces were obtained with a 30-nm bandpass filter in the $\lambda_2$ position. Eq. 2 with $n = 0.6$ was used for the intrinsic correction. (*B* and *C*) Traces of $\Delta A(\lambda, 1{:}2)$ and $\Delta A(\lambda, \delta)$ obtained from each pair of traces in *A*. Fiber 060684.2; arsenazo III concentration, 0.315–0.289 mM; additional information is given in the legend to Fig. 3*B*.

at 0° (upper trace) and 90° (lower trace) linear polarization. The 1:2 average traces (*B*) show primarily the absorbance changes that accompany Ca complexation. With the exception of the 570-nm trace, the waveforms are similar. Close inspection, however, reveals differences of the kind described in intact fibers (Baylor et al., 1983*b*; Quinta-Ferreira et al., 1984); for example, the 600-nm trace peaks slightly later than the 660-nm trace. These differences may be related to the existence of two Ca:arsenazo III complexes, possibly 1:1 and 1:2 as discussed above, that have different spectral properties and track free [Ca] with different speeds.

Panel *C* shows the dichroic traces. These traces, as well as those in *B*, are very similar in time course and wavelength dependence to traces obtained from intact fibers (Figs. 1*B*, 2*A*, and 6*A*, in Baylor et al., 1982*c*; in their Figs. 1*B* and 6*A*, an increase in absorbance was plotted as a downward deflection, the opposite of the convention used here).

*Ca-Difference Spectrum of Arsenazo III Inside Intact and Cut Muscle Fibers*

Fig. 14 compares the wavelength dependence of the early Ca signal in intact and cut fibers. Panel *A* shows results from three intact fibers. Each experimental

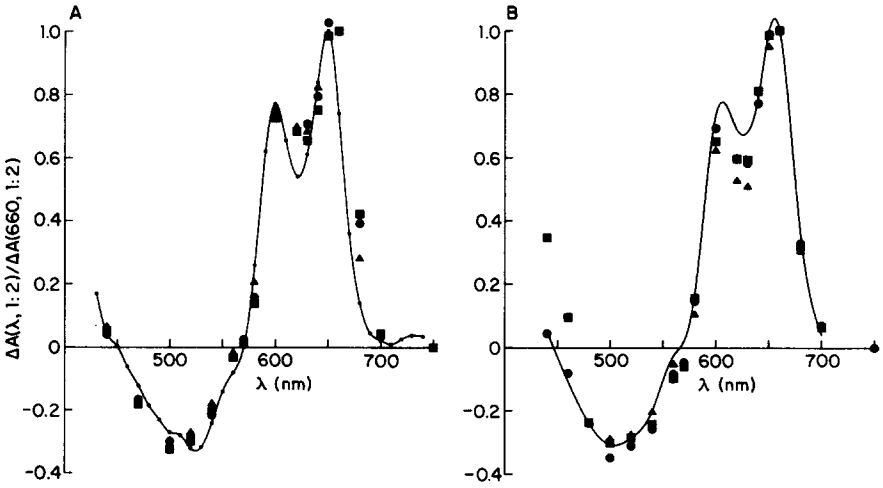


FIGURE 14. Comparison of the wavelength dependence of the rising phase of $\Delta A(\lambda, 1{:}2)$ in intact and cut muscle fibers. Each $\Delta A(\lambda, 1{:}2)$ trace, obtained using a 10-nm bandpass filter in the $\lambda_1$ position, has been fitted by the simultaneously recorded $\Delta A(660, 1{:}2)$ trace, obtained using either a 10-nm bandpass filter (intact fiber experiments) or a 30-nm bandpass filter (cut fiber experiments; trace scaled to match that obtained with a 10-nm bandpass filter) in the $\lambda_2$ position as described in the Methods. Only the initial time course, up to approximately two-thirds of the peak value of the $\lambda_2$ 660-nm trace, was used for the fit. (*A*) The larger symbols show scaling constants from three intact fibers plotted against wavelength. The small dots, connected by a continuous curve drawn using a cubic spline function (Greville, 1968), are calibration measurements, normalized by $\Delta A(650)$, taken from Fig. 7 of Baylor et al. (1982*b*), with [arsenazo III] = 0.04 $\mu$M. (*B*) Similar scaling constants obtained from three cut fibers. A cubic spline function was used to draw the continuous curve through the average values of the data points from the three intact fibers in *A*. The intact and cut fibers are the same ones used for Fig. 3 and the same symbols and arsenazo III concentrations apply.

point was obtained by scaling the simultaneously recorded $\Delta A(660, 1{:}2)$ trace to fit the $\Delta A(\lambda, 1{:}2)$ trace. Only the rising phases of the traces, to approximately two-thirds of the peak of the 660-nm signal, were used. This procedure emphasizes the earliest change in arsenazo III absorbance, which may reflect the formation of a 1:1 complex between Ca and indicator. It also minimizes possible

contributions from the slower dichroic signal. The small dots, connected by a continuous curve, were taken from the calibration measurements in Fig. 7 of Baylor et al. (1982*b*). These calibrations used a low concentration of arsenazo III, 0.04 μM, so that a large fraction of the Ca:indicator complex should be 1:1. The curve is in fair but not perfect agreement with the experimental points.

Fig. 14*B* shows comparable data from three cut fibers. The curve was drawn through the average scaled $\Delta A$ values in intact fibers, using the points in panel *A*. The agreement is good except for wavelengths between 600 and 630 nm. This discrepancy may reflect a real difference between intact and cut fibers or,

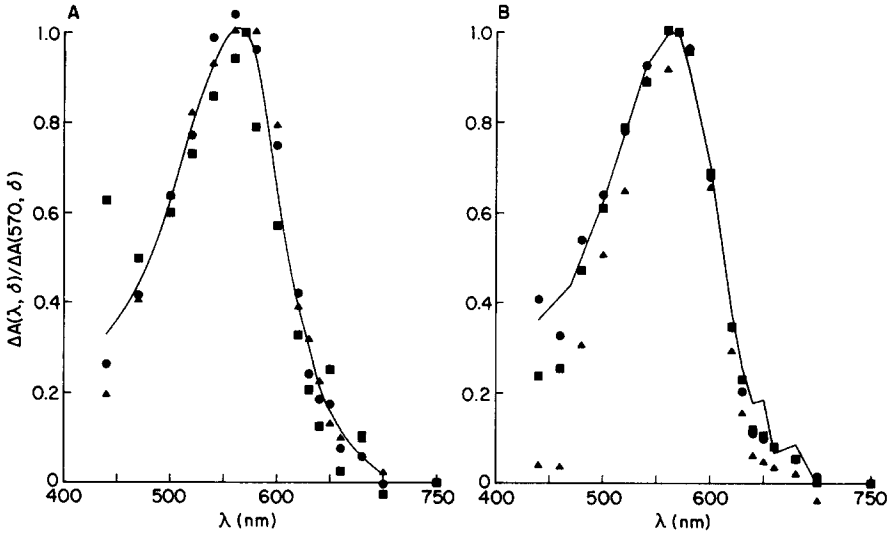


FIGURE 15. Comparison of the wavelength dependence of $\Delta A(\lambda, \delta)$ in intact and cut muscle fibers. The average of several $\Delta A(570, \delta)$ traces, taken throughout the run, has been scaled to give a least-squares fit to each $\Delta A(\lambda, \delta)$ trace. (*A*) Scaling constants from three intact fibers plotted against wavelength. The continuous curve is the average resting spectrum obtained with arsenazo III in intact muscle fibers; it is the same curve as in Fig. 3*B*. (*B*) Scaling constants from three cut fibers. Straight line segments connect the average values of data points from the three intact fibers in *A*. The intact and cut fibers are the same ones used for Fig. 3 and the same symbols and arsenazo III concentrations apply.

since 0.5–1.0 mM arsenazo III was used in the intact fiber experiments but only 0.3–0.5 mM was used in cut fibers, it may be due to an effect of indicator concentration.

### *Dichroic Spectrum of Arsenazo III Inside Intact and Cut Muscle Fibers*

Fig. 15 compares dichroic spectra in intact and cut fibers. The entire waveform of the dichroic signal at 570 nm was scaled to fit signals at other wavelengths (Fig. 13*C*). The scaling constants from intact fibers (*A*) are well fitted by the normalized resting arsenazo III absorbance curve, as first shown by Baylor et al.

(1982*c*). Panel *B* shows scaling constants obtained from cut fibers. Straight line segments connect the averaged intact fiber data from *A*. The amplitude of the dichroic signal has the same wavelength dependence in cut and intact fibers.

*Retardation Signals in Cut Fibers Containing Arsenazo III*

In intact fibers, after action potential stimulation, a change in retardation develops at about the same time that the arsenazo III Ca signal starts (Suarez-Kurtz and Parker, 1977; Baylor et al., 1982*b*). Fig. 16 shows a cut fiber

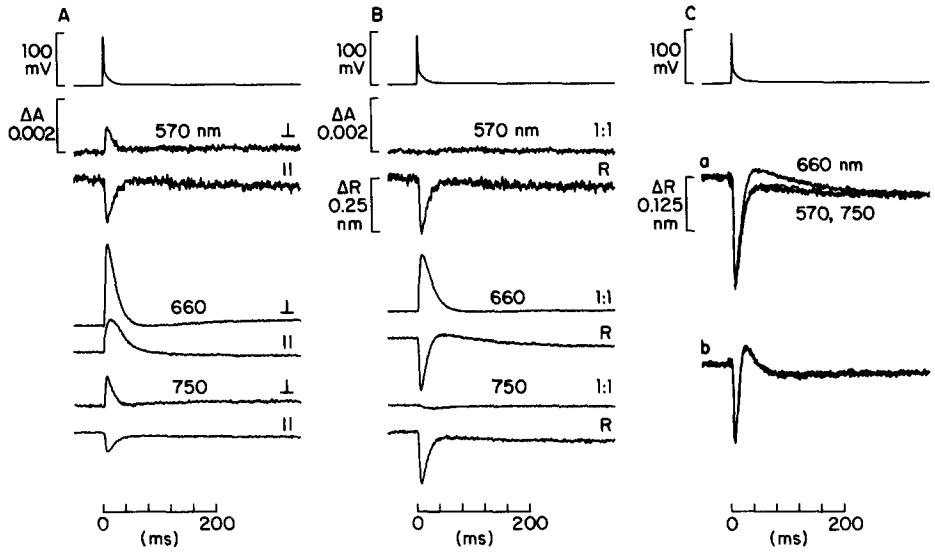


FIGURE 16. Simultaneous recording of changes in retardation and absorbance in a cut fiber containing arsenazo III. (*A*) The first trace shows the action potential and the next traces show the six changes in light transmission recorded at three wavelengths and two linear polarizations, perpendicular (⊥) and parallel (‖) to the direction of polarization of the incident light (mode 2, Irving et al., 1987). Each trace has been normalized by the resting transmitted light intensity; the vertical scale is given in absorbance units (see Fig. 11 in Irving et al., 1987). (*B*) Changes in absorbance, $\Delta A(\lambda, 1{:}1)$, and optical retardation, $\Delta R(\lambda)$, obtained from the six traces in *A* using Eqs. 6, 10, and 14 of Irving et al. (1987). No correction for the intrinsic absorbance contribution has been made in either *A* or *B*. (*C*) Part *a* shows the three retardation traces in *B*, plotted at higher gain and superimposed. The 570- and 750-nm traces are almost identical; the 570-nm trace has been smoothed (after the peak) by a 51-point quadratic routine so that the resulting less noisy trace can be distinguished from the noisier 750-nm trace. Part *b* is similar to part *a* except that the retardation traces were obtained before arsenazo III reached the site of optical recording. Fiber 100284.1; sarcomere spacing, 3.7 μm; arsenazo III concentration, 0.377 mM (*A*, *B*, and *C*, part *a*) and 0 mM (*C*, part *b*); time after saponin treatment, 75 min in *A*, *B*, and *C*, part *a*, and 30 min in *C*, part *b*; resting retardation (average of values at 570, 660, and 750 nm), 162 nm (*A*, *B*, and *C*, part *a*) and 159 nm (*C*, part *b*).

experiment in which changes in both absorbance and retardation were measured. Panel *A* shows an action potential and six optical records taken using mode 2 (Irving et al., 1987). In this mode, a change in fiber absorbance produces similar changes in the intensity of light linearly polarized perpendicular (⊥) and parallel (∥) to the direction of polarization of the incident light. On the other hand, a change in retardation produces changes in intensity that are in opposite directions on the ⊥ and ∥ traces (Irving et al., 1987). The 570- and 750-nm traces in Fig. 16*A* show a clear retardation component, similar to that observed in cut fibers without an indicator (Fig. 11 in Irving et al., 1987). The 660-nm traces have, in addition to a retardation component, a large absorbance component produced by Ca complexing with arsenazo III.

Fig. 16*B* shows $\Delta A(\lambda, 1{:}1)$ and $\Delta R(\lambda)$ signals determined from the records in *A* using Eqs. 10 and 14 in Irving et al. (1987). $\Delta A(\lambda, 1{:}1)$ was almost flat at 570 and 750 nm but showed a large change at 660 nm, as expected for the Ca signal. All three $\Delta R$ traces showed an early decrease of similar magnitude, followed by a rapid return to near baseline level. The 660-nm trace has, after the early decrease, a transient positive phase not seen at 570 or 750 nm.

Fig. 16*C* shows superimposed $\Delta R$ traces from *B* (set *a*) and from an earlier run taken before arsenazo III reached the site of optical recording (set *b*). In set *b*, the changes in retardation are independent of wavelength, in agreement with previous results on intact fibers (Baylor et al., 1984) and cut fibers that did not contain indicator (Irving et al., 1987). The traces in *a* are different from those in *b* in two ways. First, the peak of the retardation change in *a* is larger than in *b* and the waveform is altered; this is an example of the time-dependent change in the retardation signal normally observed in cut fibers (Fig. 15 in Irving et al., 1987). Second, the 660-nm trace in *a* is different from the other two superimposed traces, whereas in *b* it is the same. This difference is related to the presence of arsenazo III.

The waveform of the arsenazo III–dependent component of $\Delta R$ can be isolated from the variable fiber component by subtracting $\Delta R(750)$ from $\Delta R(660)$. Traces *a–e* in Fig. 17*A* show five such difference signals obtained at different times. Trace *a* was taken without arsenazo III (from set *b* in Fig. 16*C*), whereas *b–e* were taken as arsenazo III diffused into the fiber; *d* is from set *a* in Fig. 16*C*. Since the fiber contribution to $\Delta R(660)$ and $\Delta R(750)$ should be the same, these $\Delta R$ difference traces represent indicator-related changes in retardation.

According to the Kramers-Kronig relation (Fredericq and Houssier, 1973), an indicator-related dichroic signal should produce an indicator-related retardation signal, as found in squid axons stained with certain membrane potential–sensitive dyes (Ross et al., 1977; Gupta et al., 1981). Thus, the arsenazo III dichroic signal would be expected to produce an indicator-related retardation signal. If signals *b–e* in Fig. 17 originate by this mechanism, they should have the same time course as the dichroic signal and the same dependence on the arsenazo III concentration.

The peak amplitude of $\Delta R(660) - \Delta R(750)$ is plotted against the arsenazo III concentration in Fig. 17*B*. The variation with concentration is similar to that shown by the dichroic signal (Fig. 6*C*). The curve, calculated from the 1:1

binding isotherm (Eq. 12), provides a reasonable fit to the data with a $K_D$ value of 4.7/cm, which is similar to that obtained for dichroic signals (Table IV, column 3).

After retardation traces *a–e* in Fig. 17*A* were obtained, the polarizer was removed and the fiber was rotated for mode 1 recording. The uppermost optical trace in Fig. 17*A* shows a dichroic signal recorded soon thereafter. Its time course is similar to that of arsenazo III–related retardation (trace *e*), except for the early downward component in *e*.

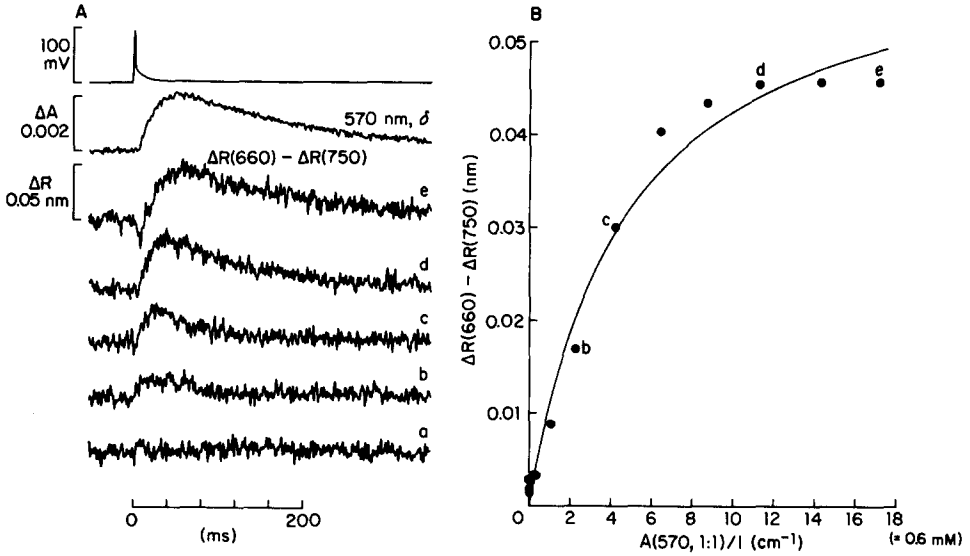


FIGURE 17. Effect of arsenazo III concentration on the difference signal $\Delta R(660) - \Delta R(750)$. (*A*) The first trace is an action potential; the second trace is $\Delta A(570, \delta)$ recorded in mode 1 after the traces in mode 2 were taken, [arsenazo III] = 0.9 mM; the next five traces are $\Delta R(660) - \Delta R(750)$ taken at different times as indicator was diffusing into the fiber, mode 2 recording. The trace marked *a* was obtained from Fig. 16*C*, part *b*, [arsenazo III] = 0 mM. Traces *b–e* were taken as arsenazo III diffused to the site of optical recording. Trace *d* is from the records shown in Fig. 16 *C*, part *a*. (*B*) Peak amplitude of $\Delta R(660) - \Delta R(750)$ plotted against $A(570, 1:1)/l$, or indicator concentration. The continuous curve represents a least-squares fit of Eq. 12, with $K_D$ = 4.7/cm (which corresponds to an indicator concentration of 0.16 mM) and a maximum value of 0.062 nm for $\Delta R(660) - \Delta R(750)$. Resting retardation (average value at 570, 660, and 750 nm) = 159 (*a*), 161 (*b*), 161 (*c*), 162 (*d*), and 163 (*e*) nm. Other fiber information is given in the legend to Fig. 16.

The origin of this component is unknown. One possibility is contamination by the Ca signal. The amount of contamination would depend on the amplitude of $\Delta A(660, 1:1)$ and would therefore increase with increasing indicator concentration. This would be consistent with trace *e* in Fig. 17*A* having the largest early downward component. If this explanation is correct, it indicates that the method used to eliminate absorbance changes from $\Delta R$ signals does not work perfectly.

One possible source of error is that the theory for determining $\Delta R$ is based on a constant optical path length, whereas the incident light forming the 50-$\mu$m spot, with numerical aperture 0.4, is expected to have a variable path length in the fiber.

In traces *b–e* in Fig. 17*A*, the time to peak progressively increased as arsenazo III diffused into the fiber. A similar effect of indicator concentration was consistently found in dichroic signals in cut fibers (not shown) and intact fibers (Fig. 8 in Baylor et al., 1982*c*).

The expected magnitude of the arsenazo III–related retardation signal can be calculated by numerical evaluation of the Kramers-Kronig relation (Emeis et al., 1967). The calculation requires knowing the spectral dependence of the dichroic absorbance change and its amplitude. The resting absorbance spectrum for arsenazo III (Fig. 3*B*) was used for the spectral dependence since it matches that of the dichroic signal (Fig. 15). The peak value of $\Delta A(570, \delta)$ in Fig. 17*A*, $2.07 \times 10^{-3}$, predicts peak values of the arsenazo III–related $\Delta R$ of +0.061, +0.125, and +0.072 nm at 570, 660, and 750 nm, respectively. Thus, according to the numerical evaluation of the Kramers-Kronig relation, $\Delta R$ should be more positive at 660 nm than at 570 or 750 nm, in agreement with set *a* of Fig. 16*C*, and the predicted peak value of $\Delta R(660) - \Delta R(750)$ should be 0.053 nm, in agreement with the observed value of 0.046 nm recorded earlier in the experiment (Fig. 17*A*, trace *e*).

The experiment in Figs. 16 and 17 shows that the arsenazo III–related retardation signal is produced by the arsenazo III–related dichroic signal. The ability to resolve such a signal provides a successful test of both the apparatus and the theory for its use in mode 2.

### *Arsenazo III Ca Signals and Changes in Retardation after Single Stimulation and Multiple Stimulation*

Baylor et al. (1982*b*, 1984) showed that the rising phases of the retardation signal and the arsenazo III Ca signal virtually superimpose after action potential stimulation of an intact fiber. Fig. 18*A* shows that the same relation holds in cut fibers. The $\Delta A(660, 1{:}1)$ and $\Delta R(750)$ traces follow similar time courses early in the transient but become different later, so that the retardation trace has a shorter half-width.

Panels *B* and *C* of Fig. 18 compare the Ca and retardation signals that accompany 1 and 10 action potentials. During 100 Hz stimulation, the Ca signal (middle set of traces) summated, as in intact fibers (Baylor et al., 1982*c*; Miledi et al., 1982). Since summation is not generally observed with antipyrylazo III (Maylie et al., 1987), it is probably not produced by a progressive increase in free [Ca]; it is more likely to be due to the slow component of the arsenazo III Ca signal (Baylor et al., 1983*b*; Quinta-Ferreira et al., 1984). The small maintained increase in absorbance (*C*) could be produced by an increase in Ca, pH, or Mg, either alone or in combination.

Changes in retardation are shown in the lowermost traces in Fig. 18, *B* and *C*. 10 action potentials produced summation of both peak and maintained levels. Repetitive stimulation was used in two other mode 2 experiments with variable

results: in one fiber (which contained the pH indicator phenol red), the peak but not the steady level summated, whereas in the other fiber (which contained antipyrylazo III, Fig. 16 in Maylie et al., 1987), the steady level but not the peak summated.

The retardation change after repetitive stimulation persisted for a considerable period of time. In another experiment (on the fiber that contained phenol red), a much slower sampling rate was used and the late change was found to be

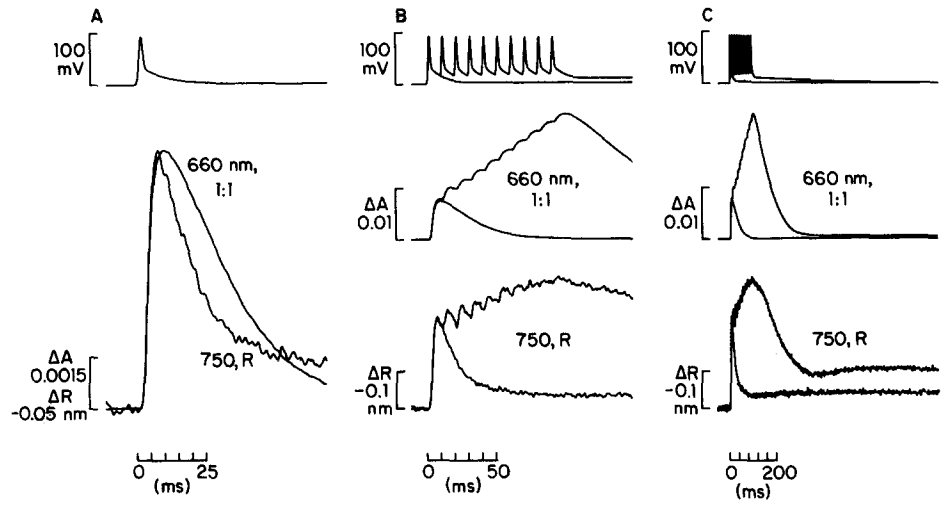


FIGURE 18. Comparison of Ca and retardation signals in a cut fiber containing arsenazo III. (*A*) Traces associated with a single action potential. The top record shows the action potential and the two superimposed traces show $\Delta A(660, 1{:}1)$ and $\Delta R(750)$ scaled so that the peaks match. The retardation trace has been inverted to facilitate comparison with the Ca signal. (*B* and *C*) Comparison of traces associated with 1 and 10 action potentials plotted on fast and slow time bases, respectively. The top pair of superimposed traces shows the action potentials, the middle pair shows $\Delta A(660, 1{:}1)$, and the bottom pair shows $\Delta R(750)$. The single action potential traces are the same as in *A*. The intrinsic correction used Eq. 2 with $n = 1.0$. Same experiment as Figs. 15 and 16; arsenazo III concentration, 0.75 mM; time after saponin treatment, 91–92 min.

maintained for 8 s (not shown). Similar maintained changes may occur in intact fibers, although as far as we are aware, their existence has not yet been reported.

As mentioned in the previous section, the $\Delta R(750)$ traces should include a component causally related to the arsenazo III dichroic signal. According to the Kramers-Kronig relation, the magnitude of this component should be about +0.07 nm after a single action potential; its positive amplitude, opposite to that of the intrinsic retardation signal, should abbreviate the $\Delta R(750)$ signal after a single action potential (Fig. 18*A*). This component should also contribute to $\Delta R(750)$ after 10 action potentials, but, since the dichroic signal plateaus after one to two action potentials (Baylor et al., 1982*c*), its contribution should be fairly constant (Fig. 18, *B* and *C*).

*Arsenazo III Ca Signals Recorded Near Threshold under Voltage Clamp*

In intact fibers, the amplitude of the arsenazo III Ca signal, near threshold, is steeply voltage dependent, increasing e-fold for each additional 3–4 mV of depolarization (Baylor et al., 1979, 1983*a*; Miledi et al., 1981). Intramembranous charge movement, a candidate for the voltage sensor in excitation-contraction coupling, occurs in the voltage range where contraction is activated. Since its

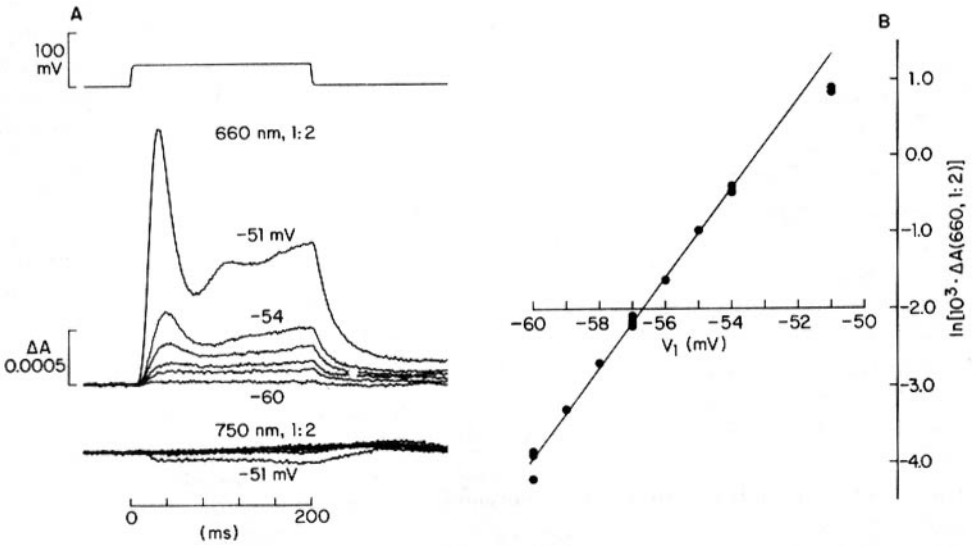


FIGURE 19. Arsenazo III Ca signals recorded near threshold under voltage clamp. (*A*) The top trace shows a single depolarizing voltage pulse from a holding potential of −90 mV. The middle set of traces shows $\Delta A(660, 1{:}2)$ associated with pulses to six different voltages, −60, −57, −56, −55, −54, and −51 mV; the optical traces became progressively larger as the potential was made more positive. The intrinsic correction for each 660-nm trace used the corresponding 750-nm trace, smoothed by a 51-point quadratic routine, and scaled according to Eq. 2 with $n = 1.0$. The bottom set shows the smoothed $\Delta A(750, 1{:}2)$ traces. (*B*) Peak $\Delta A(660, 1{:}2)$ has been plotted semilogarithmically against voltage during the step, from traces in *A* and other measurements from the same experiment. The straight line represents a least-squares fit to all data points except the two at −51 mV; its slope corresponds to an e-fold increase every 1.7 mV. Fiber 101284.2; sarcomere spacing, 4.0 μm; arsenazo III concentration, 0.827–0.844 mM; time after saponin treatment, 72–90 min.

voltage dependence appears to be less steep in cut than in intact fibers (see Introduction), it seemed of interest to measure the voltage dependence of the Ca signal in cut fibers to find out whether it, too, is less steep.

Fig. 19 shows results from one of two experiments. The top record in *A* shows a 200-ms step depolarization. The next six superimposed traces show the arsenazo III Ca signal associated with steps to −60 to −51 mV from a holding potential of −90 mV; the middle four traces were taken at 1-mV intervals from −57 to −54 mV. After the smallest depolarizations, the Ca signal, after an initial delay, reached a relatively constant level. At larger depolarizations, however, it showed

an early peak, which at −51 mV was followed by a slight oscillatory phase. Waveforms such as these will be discussed in the following article (Maylie et al., 1987), which contains additional results from antipyrylazo III experiments. The lower set of six traces shows the relatively small intrinsic signals that were used to correct the 660-nm traces.

In Fig. 19*B*, the peak amplitude of the Ca signal has been plotted on a semilogarithmic scale as a function of membrane potential. The straight line corresponds to an e-fold change every 1.7 mV. Another fiber gave an e-fold change every 1.8 mV. Thus, both cut fibers had steep $\Delta A(660)$ vs. voltage relations, in fact steeper than those reported in the few experiments carried out on intact fibers (although more experiments would be required to determine whether this difference is real). It does seem clear, however, that in contrast to previous studies of charge movement and the Nile Blue A fluorescence signal (see Introduction), the voltage dependence of the Ca signal in cut fibers is not less steep than that in intact fibers.

The traces in Fig. 19*A* were taken 72–90 min after saponin treatment. Another set of traces was taken 257–265 min after treatment. During the interval, the relation between the peak amplitude of the Ca signal and voltage had become less steep and was shifted several millivolts in the negative direction on the voltage axis; the e-fold factor changed from the initial value of 1.7 mV to 2.4 mV. In the other voltage-clamp experiment, the records that gave an e-fold change for 1.8 mV were taken 52–58 min after saponin treatment. The final set of records, taken 268–277 min after saponin treatment, gave an e-fold change for 3.2 mV. As before, the relation between the peak amplitude of the Ca signal and voltage was shifted several millivolts in the negative direction.

These results and similar ones obtained with antipyrylazo III (Maylie et al., 1987) show that the amplitude of Ca signals in cut fibers can show steep voltage dependence, at least as steep as that reported for intact fibers, but that the exact relation between peak Ca and membrane potential may change during the course of a long experiment.

## DISCUSSION

One of the new findings described above is that the concentration of arsenazo III at the optical recording site in the center of a cut fiber can reach two to three times that present in the end pools. Thus, arsenazo III appears to be bound to or taken up by intracellular constituents or compartments. The time course of indicator diffusion into fibers can be fitted by theoretical predictions derived from free diffusion plus linear reversible binding (Eqs. 6 and 8). These fits indicate that, on average, 73% of the arsenazo III is bound. Another new finding is that if indicator is removed from the end pools after a brief exposure (0.4–0.9 h), it remains inside the fiber longer than diffusion plus reversible binding predicts. But if the diffusion theory is extended to include both linear reversible and linear irreversible binding (Eqs. 10 and 11), the complete time course can be fitted.

A consequence of the extended theory is that it may require that irreversibly bound indicator be able to react with Ca. In experiments in which indicator diffuses into and out of a fiber, the relationship between peak $\Delta A(660, 1{:}2)$ and

the indicator concentration is frequently reversible. Thus, at *b* and *d* in Fig. 6*A*, the concentration of arsenazo III was nearly the same and so was the amplitude of the Ca signal. According to the theory, only a small amount of arsenazo III was irreversibly bound when measurement *b* was made, whereas slightly more than three-quarters was irreversibly bound when measurement *d* was made (Fig. 2*B*). Either irreversibly bound arsenazo III was able to react with Ca or peak free [Ca] increased by the amount required to make the peak in *d* match that in *b*. Alternatively, the assumptions about binding and diffusion may be incorrect; for example, $D$ or $R$ may change with time or binding may not be linear or instantaneous.

The discovery of bound arsenazo III should come as no surprise. Beeler et al. (1980) reported such binding in subcellular fractions isolated from rabbit muscle and studied at 4°C. They predicted that the bound fraction would be 0.8–0.9 inside a fiber containing a total concentration of 1–2 mM arsenazo III. This fractional amount is similar to that obtained from our diffusion analysis, 0.73 if reversible binding is assumed [$= R/(R + 1)$, column 5 of Table II] or a lower limit of 0.82 if reversible plus irreversible binding is assumed (0.82 is the reversible fraction, column 3 of Table III). With binding taken into account, the free diffusion constant is calculated, on average, to be $0.859 \times 10^{-6}$ cm$^2$/s for reversible binding (Table II, column 6) and $1.089 \times 10^{-6}$ cm$^2$/s for reversible plus irreversible binding (Table III, column 4). These values seem consistent with the value $1.2 \times 10^{-6}$ cm$^2$/s for ATP, 507 mol wt compared with 776 for arsenazo III, obtained by Kushmerick and Podolsky (1969) for diffusion in skinned muscle fibers at 20°C. Thus, our values of $(R + 1)$ and $D$, determined from the time course of arsenazo III concentration, are in satisfactory agreement with the values expected from other studies.

There is no direct information about arsenazo III binding in intact fibers. It probably does occur, because the apparent diffusion constant is small, $0.12 \times 10^{-6}$ cm$^2$/s in highly stretched fibers at 16°C (Baylor et al., 1986). This value, which should equal $D/(R + 1)$, is somewhat smaller than the average cut fiber values, $0.237 \times 10^{-6}$ cm$^2$/s (Table II, column 4) and $0.211 \times 10^{-6}$ cm$^2$/s (Table III, column 2).

The present work also shows that, although Ca signals in freshly prepared cut fibers are similar to those in intact fibers, they change as cut fiber experiments progress. For example, the half-width of the Ca signal produced by action potential stimulation increases with time. This happens whether the indicator concentration is increasing or decreasing. Another change is that the relation between peak amplitude of the Ca signal and voltage becomes somewhat less steep and is shifted to more negative potentials. Since these effects are also observed with antipyrylazo III, a more reliable indicator for measuring myoplasmic Ca transients (Baylor et al., 1983*b*; Quinta-Ferreira et al., 1984), their significance in terms of progressive changes in the internal state of cut fibers (see Irving et al., 1987) will be discussed after the experiments with antipyrylazo III have been described (Maylie et al., 1987).

We thank the staff of the Yale Department of Physiology Electronics Laboratory for help with the design and construction of equipment. We owe special thanks to Dr. S. M. Baylor for telling

us early on about his results with arsenazo III and to Dr. L. B. Cohen for continual helpful discussion. We also thank Drs. Baylor and Cohen for their useful comments on the manuscript.

This work was supported by the U.S. Public Health Service grants NS-07474 and AM-37643. M.I. was initially a Science and Engineering Research Council Postdoctoral Fellow and subsequently a Royal Society University Research Fellow.

*Original version received 5 May 1986 and accepted version received 15 September 1986.*

## REFERENCES

Adrian, R. H., and W. Almers. 1976. Charge movement in the membrane of striated muscle. *Journal of Physiology.* 254:339–360.

Baylor, S. M., W. K. Chandler, and M. W. Marshall. 1979. Arsenazo III signals in singly dissected frog twitch fibres. *Journal of Physiology.* 287:23P–24P.

Baylor, S. M., W. K. Chandler, and M. W. Marshall. 1982*a*. Optical measurements of intracellular pH and magnesium in frog skeletal muscle fibres. *Journal of Physiology.* 331:105–137.

Baylor, S. M., W. K. Chandler, and M. W. Marshall. 1982*b*. Use of metallochromic dyes to measure changes in myoplasmic calcium during activity in frog skeletal muscle fibres. *Journal of Physiology.* 331:139–177.

Baylor, S. M., W. K. Chandler, and M. W. Marshall. 1982*c*. Dichroic components of Arsenazo III and Dichlorophosphonazo III signals in skeletal muscle fibres. *Journal of Physiology.* 331:179–210.

Baylor, S. M., W. K. Chandler, and M. W. Marshall. 1983*a*. Sarcoplasmic reticulum calcium release in frog skeletal muscle fibres estimated from Arsenazo III calcium transients. *Journal of Physiology.* 344:625–666.

Baylor, S. M., M. E. Quinta-Ferreira, and C. S. Hui. 1983*b*. Comparison of isotropic calcium signals from intact frog muscle fibers injected with Arsenazo III or Antipyrylazo III. *Biophysical Journal.* 44:107–112.

Baylor, S. M., W. K. Chandler, and M. W. Marshall. 1984. Calcium release and sarcoplasmic reticulum membrane potential in frog skeletal muscle fibres. *Journal of Physiology.* 348:209–238.

Baylor, S. M., S. Hollingworth, C. S. Hui, and M. E. Quinta-Ferreira. 1986. Properties of the metallochromic dyes Arsenazo III, Antipyrylazo III and Azo1 in frog skeletal muscle fibres at rest. *Journal of Physiology.* 377:89–141.

Beeler, T. J., A. Schibeci, and A. Martonosi. 1980. The binding of Arsenazo III to cell components. *Biochimica et Biophysica Acta.* 629:317–327.

Brown, J. E., L. B. Cohen, P. De Weer, L. H. Pinto, W. N. Ross, and B. M. Salzberg. 1975. Rapid changes of intracellular free calcium concentration: detection by metallochromic indicator dyes in squid giant axon. *Biophysical Journal.* 15:1155–1160.

Chandler, W. K., R. F. Rakowski, and M. F. Schneider. 1976. A non-linear voltage dependent charge movement in frog skeletal muscle. *Journal of Physiology.* 254:245–283.

Crank, J. 1956. The Mathematics of Diffusion. Clarendon Press, Oxford. 347 pp.

Emeis, C. A., L. J. Oosterhoff, and G. d. Vries. 1967. Numerical evaluation of Kramers-Kronig relations. *Proceedings of the Royal Society of London, Series A.* 297:54–65.

Fredericq, E., and C. Houssier. 1973. Electric Dichroism and Electric Birefringence. Clarendon Press, Oxford. 7–59.

Greville, T. N. E. 1968. Spline functions, interpolation, and numerical quadrature. *In* Mathe-

matical Methods for Digital Computers. A. Ralston and H. S. Wilf, editors. John Wiley & Sons, Inc., New York. 156–168.

Gupta, R. K., B. M. Salzberg, A. Grinvald, L. B. Cohen, K. Kamino, S. Lesher, M. B. Boyle, A. S. Waggoner, and C. H. Wang. 1981. Improvements in optical methods for measuring rapid changes in membrane potential. *Journal of Membrane Biology.* 58:123–137.

Horowicz, P., and M. F. Schneider. 1981. Membrane charge movement in contracting and non-contracting skeletal muscle fibres. *Journal of Physiology.* 314:565–593.

Hui, C. S. 1983. Pharmacological studies of charge movement in frog skeletal muscle. *Journal of Physiology.* 337:509–529.

Irving, M., J. Maylie, N. L. Sizto, and W. K. Chandler. 1987. Passive electrical and intrinsic optical properties of cut frog twitch fibers. *Journal of General Physiology.* 89:1–40.

Kendrick, N. C., R. W. Ratzlaff, and M. P. Blaustein. 1977. Arsenazo III as an indicator for ionized calcium in physiological salt solutions: its use for determination of the CaATP dissociation constant. *Analytical Biochemistry.* 83:433–450.

Kovacs, L., and M. F. Schneider. 1978. Contractile activation by voltage clamp depolarization of cut skeletal muscle fibres. *Journal of Physiology.* 277:483–506.

Kushmerick, M. J., and R. J. Podolsky. 1969. Ionic mobility in muscle cells. *Science.* 166:1297–1298.

Luttgau, H. C., G. Gottschalk, L. Kovacs, and M. Fuxreiter. 1983. How perchlorate improves excitation-contraction coupling in skeletal muscle fibers. *Biophysical Journal.* 43:247–249.

Maylie, J., M. Irving, N. L. Sizto, and W. K. Chandler. 1987. Calcium signals recorded from cut frog twitch fibers containing antipyrylazo III. *Journal of General Physiology.* 89:83–143.

Miledi, R., S. Nakajima, I. Parker, and T. Takahashi. 1981. Effects of membrane polarization on sarcoplasmic calcium release in skeletal muscle. *Proceedings of the Royal Society of London, Series B.* 213:1–13.

Miledi, R., I. Parker, and G. Schalow. 1977. Measurement of calcium transients in frog muscle by the use of arsenazo III. *Proceedings of the Royal Society of London, Series B.* 198:201–210.

Miledi, R., I. Parker, and P. H. Zhu. 1982. Calcium transients evoked by action potentials in frog twitch muscle fibres. *Journal of Physiology.* 333:655–679.

Palade, P., and J. Vergara. 1981. Detection of Ca with optical methods. *In* The Regulation of Muscle Contraction: Excitation-Contraction Coupling. A. D. Grinnell and M. A. B. Brazier, editors. Academic Press, Inc., New York. 143–158.

Palade, P., and J. Vergara. 1983. Stoichiometries of Arsenazo III-Ca complexes. *Biophysical Journal.* 43:355–369.

Pappone, P. A. 1980. Voltage-clamp experiments in normal and denervated mammalian skeletal muscle fibres. *Journal of Physiology.* 306:377–410.

Quinta-Ferreira, M. E., S. M. Baylor, and C. S. Hui. 1984. Antipyrylazo III (Ap III) and Arsenazo III (Az III) calcium transients from frog skeletal muscle fibers simultaneously injected with both dyes. *Biophysical Journal.* 45:47*a*. (Abstr.)

Rios, E., and M. F. Schneider. 1981. Stoichiometry of the reactions of calcium with the metallochromic indicator dyes Antipyrylazo III and Arsenazo III. *Biophysical Journal.* 36:607–621.

Ross, W. N., B. M. Salzberg, L. B. Cohen, A. Grinvald, H. V. Davila, A. S. Waggoner, and C. H. Wang. 1977. Changes in absorption, fluorescence, dichroism, and birefringence in stained giant axons: optical measurement of membrane potential. *Journal of Membrane Biology.* 33:141–183.

Schneider, M. F., and W. K. Chandler. 1973. Voltage dependent charge movement in skeletal muscle: a possible step in excitation-contraction coupling. *Nature.* 242:244–246.

Schneider, M. F., and W. K. Chandler. 1976. Effects of membrane potential on the capacitance of skeletal muscle fibers. *Journal of General Physiology.* 67:125–163.

Shlevin, H. H. 1979. Effects of external calcium concentration and pH on charge movement in frog skeletal muscle. *Journal of Physiology.* 288:129–158.

Suarez-Kurtz, G., and I. Parker. 1977. Birefringence signals and calcium transients in skeletal muscle. *Nature.* 270:746–748.

Thomas, M. V. 1979. Arsenazo III forms 2:1 complexes with Ca and 1:1 complexes with Mg under physiological conditions. *Biophysical Journal.* 25:541–548.

Vergara, J., F. Bezanilla, and B. M. Salzberg. 1978. Nile Blue fluorescence signals from cut single muscle fibers under voltage or current clamp conditions. *Journal of General Physiology.* 72:775–800.

Yingst, D. R., and J. F. Hoffman. 1978. Changes of intracellular Ca as measured by Arsenazo III in relation to the K permeability of human erythrocyte ghosts. *Biophysical Journal.* 23:463–471.